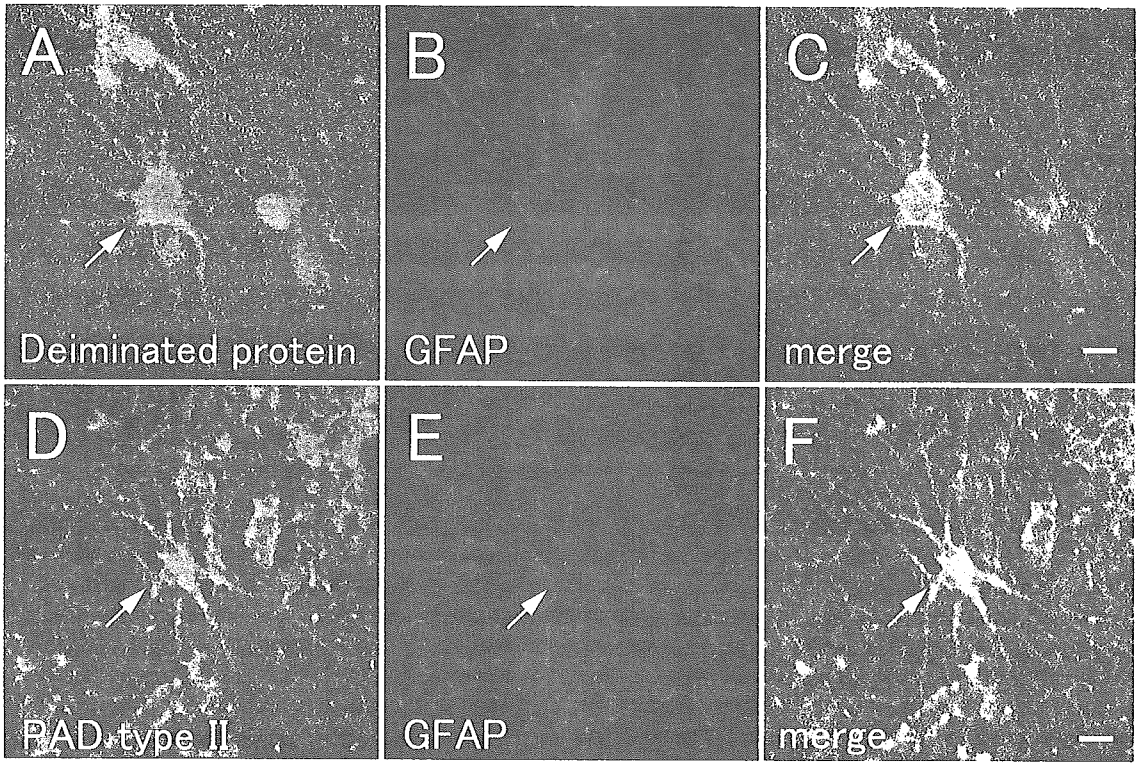

Fig. 5. Identification of citrullinated protein-positive and PAD2-positive cells by double immunofluorescence staining. Sections of AD hippocampus were doubly immunostained with monoclonal anti-GFAP antibody and with polyclonal antimodified citrulline IgG or polyclonal anti-human PAD2 antibody. The primary antibodies were visualized with anti-rabbit Alexa Fluor 488 (green) and anti-mouse Alexa Fluor 594 (red). **A,D:** Alexa 488 (green) for citrullinated protein (A) or PAD2 (D). **B,E:** Alexa 568 (red) for GFAP. **C,F:** Merged views for A/B and D/E, respectively. Arrows indicate coincident position. Scale bars = 5 μm.

important functions in the brains of AD patients. Inagaki et al. (1989) reported that vimentin and GFAP were highly susceptible to the attack of PAD2 in vitro; for example, citrullination of vimentin induced disassembly of intermediate filaments.

Here, we also identified citrullinated MBP, which is an authentic marker of oligodendrocyte, in the AD-afflicted hippocampus. Recently, we found PAD2 localized in a stage-specific, immature oligodendrocyte from a rat's cerebral hemisphere in vitro (Akiyama et al., 1999). Gould et al. (2000) reported that PAD2 cDNA was highly expressed in myelin sheath assembly sites with a combination of subcellular fractionation and suppression subtractive hybridization. Moreover, Moscarello et al. (1994, 2002) reported that PAD enzyme and citrullinated MBP are relatively enriched in immature myelin and that MBP citrullination has an important role in myelin development and in the human demyelinating disease multiple sclerosis. Recently, many investigators have suggested that myelin breakdown may be a contributing factor in the pathology of AD (Bartzokis, 2004; Tian et al., 2004). MBP citrullination might also contribute to the myelin breakdown.

The mechanism(s) by which citrullinated proteins occur in the hippocampus during AD remains unclear. Possibly PAD2 becomes activated, abundant, and functional only in the presence of AD, insofar as the amount of PAD2 increased notably in hippocampi of the AD patients we assessed compared with that in normal subjects. Although PAD2 was also present in hippocampal extracts from normal subjects, that enzyme remained in a steady state during which no enzyme activation occurred. For enzyme activation, the intracellular calcium concentration must become elevated. No other factors can regulate PAD activity in vivo or in vitro, to the best of our knowledge. A loss of neuronal calcium homeostasis leading to increases in the intracellular calcium concentration has been proposed to play a major role in hypoxic and ischemic brain injury (Choi, 1988; Hossmann, 1999). Haun et al. (1992) suggested that an influx of extracellular calcium contributes to astroglial injury during ischemia on the basis of their experimental results with simulated ischemia in a primary culture of astrocytes. Our previous report showed that PAD2 activated and citrullinated various cerebral proteins under hypoxic conditions (Asaga and Ishigami, 2000) and during kainic acid-evoked neurodegeneration (Asaga and Ishigami, 2001; Asaga et al., 2002). Abnormal PAD activation resulted in random protein citrullination, which could then trigger the onset of neurodegenerative disease.

In conclusion, the present data indicate that patients with AD bear an abnormal accumulation of citrullinated

proteins and abnormal activation of PAD2 in the hippocampus. Therefore, citrullinated proteins may be a useful marker for neurodegenerative disease. Moreover, the development of an inhibitory drug specific for PAD2 could conceivably prevent the onset and progression of neurodegeneration.

ACKNOWLEDGMENTS

The excellent editorial assistance of Ms. P. Minick is gratefully acknowledged. This study was supported by a Grant-in-Aid for Scientific Research from the Ministry of Education, Science, and Culture, Japan (to A.I.) and a grant from Health Science Research Grants for Comprehensive Research on Aging and Health supported by the Ministry of Health Labor and Welfare, Japan (to A.I.). Additional support was provided by the SHISEIDO Grant for Scientific Research (to A.I.), the Cosmetology Research Foundation (to A.I.), and the Nakatomi Foundation (to A.I.).

REFERENCES

Akiyama K, Sakurai Y, Asou H, Senshu T. 1999. Localization of peptidylarginine deiminase type II in a stage-specific immature oligodendrocyte from rat cerebral hemisphere. Neurosci Lett 274:53–55.

Asaga H, Ishigami A. 2000. Protein deimination in the rat brain: generation of citrulline-containing proteins in cerebrum perfused with oxygen-deprived media. Biomed Res 21:197–205.

Asaga H, Ishigami A. 2001. Protein deimination in the rat brain after kainate administration: citrulline-containing proteins as a novel marker of neurodegeneration. Neurosci Lett 299:5–8.

Asaga H, Senshu T. 1993. Combined biochemical and immunocytochemical analyses of postmortem protein deimination in the rat spinal cord. Cell Biol Int 17:525–532.

Asaga H, Akiyama K, Ohsawa T, Ishigami A. 2002. Increased and type II-specific expression of peptidylarginine deiminase in activated microglia but not hyperplastic astrocytes following kainic acid-evoked neurodegeneration in the rat brain. Neurosci Lett 326:129–132.

Bartzokis G. 2004. Age-related myelin breakdown: a developmental model of cognitive decline and Alzheimer's disease. Neurobiol Aging 25: 5–18.

Chavanas S, Mechin MC, Takahara H, Kawada A, Nachat R, Serre G, Simon M. 2004. Comparative analysis of the mouse and human peptidylarginine deiminase gene clusters reveals highly conserved non-coding segments and a new human gene, PADI6. Gene 330:19–27.

Choi DW. 1988. Calcium-mediated neurotoxicity: relationship to specific channel types and role in ischemic damage. Trends Neurosci 11:465–469.

Gould RM, Freund CM, Palmer F, Feinstein DL. 2000. Messenger RNAs located in myelin sheath assembly sites. J Neurochem 75:1834–1844.

Haun SE, Murphy EJ, Bates CM, Horrocks LA. 1992. Extracellular calcium is a mediator of astroglial injury during combined glucose-oxygen deprivation. Brain Res 593:45–50.

Hossmann KA. 1999. The hypoxic brain. Insights from ischemia research. Adv Exp Med Biol 474:155–169.

Imparl JM, Senshu T, Graves DJ. 1995. Studies of calcineurin-calmodulin interaction: probing the role of arginine residues using peptidylarginine deiminase. Arch Biochem Biophys 318:370–377.

Inagaki M, Takahara H, Nishi Y, Sugawara K, Sato C. 1989. Ca^{2+}-dependent deimination-induced disassembly of intermediate filaments involves specific modification of the amino-terminal head domain. J Biol Chem 264:18119–18127.

Ishigami A, Ohsawa T, Watanabe K, Senshu T. 1996. All-trans retinoic acid increases peptidylarginine deiminases in a newborn rat keratinocyte cell line. Biochem Biophys Res Commun 223:299–303.

Ishigami A, Kuramoto M, Yamada M, Watanabe K, Senshu T. 1998. Molecular cloning of two novel types of peptidylarginine deiminase cDNAs from retinoic acid-treated culture of a newborn rat keratinocyte cell line. FEBS Lett 433:113–118.

Ishigami A, Asaga H, Ohsawa T, Akiyama K, Maruyama N. 2001. Peptidylarginine deiminase type I, type II, type III and type IV are expressed in rat epidermis. Biomed Res 22:63–65.

Ishigami A, Asaga H, Ohsawa T, Akiyama K, Maruyama N. 2002a. Protein deimination and peptidylarginine deiminase expression during cornification of rat epidermal keratinocytes. Biomed Res 23:145–151.

Ishigami A, Ohsawa T, Asaga H, Akiyama K, Kuramoto M, Maruyama N. 2002b. Human peptidylarginine deiminase type II: molecular cloning, gene organization, and expression in human skin. Arch Biochem Biophys 407:25–31.

Katzman R. 1986. Alzheimer's disease. N Engl J Med 314:964–973.

Keller JN, Hanni KB, Markesbery WR. 2000. Impaired proteasome function in Alzheimer's disease. J Neurochem 75:436–439.

Kubilus J, Baden HP. 1983. Purification and properties of a brain enzyme which deiminates proteins. Biochim Biophys Acta 745:285–291.

Kubilus J, Waitkus RF, Baden HP. 1980. Partial purification and specificity of an arginine-converting enzyme from bovine epidermis. Biochim Biophys Acta 615:246–251.

Laemmli UK. 1970. Cleavage of structural proteins during the assembly of the head of bacteriophage T4. Nature 227:680–685.

Lamensa JW, Moscarello MA. 1993. Deimination of human myelin basic protein by a peptidylarginine deiminase from bovine brain. J Neurochem 61:987–996.

Lowry OH, Rosebrough NJ, Farr AL, Randall RJ. 1951. Protein measurement with the phenol reagent. J Cell Biol 193:265–275.

Maccioni RB, Munoz JP, Barbeito L. 2001. The molecular bases of Alzheimer's disease and other neurodegenerative disorders. Arch Med Res 32:367–381.

Moscarello MA, Wood DD, Ackerley C, Boulias C. 1994. Myelin in multiple sclerosis is developmentally immature. J Clin Invest 94:146–154.

Moscarello MA, Pritzker L, Mastronardi FG, Wood DD. 2002. Peptidylarginine deiminase: a candidate factor in demyelinating disease. J Neurochem 81:335–343.

Nakashima K, Hagiwara T, Ishigami A, Nagata S, Asaga H, Kuramoto M, Senshu T, Yamada M. 1999. Molecular characterization of peptidylarginine deiminase in HL-60 cells induced by retinoic acid and 1α, 25-dihydroxyvitamin D_3. J Biol Chem 274:27786–27792.

National Institute on Aging, and Reagan Institute Working Group on Diagnostic Criteria for the Neuropathological Assessment of Alzheimer's Disease. 1997. Consensus recommendations for the postmortem diagnosis of Alzheimer's disease. Neurobiol Aging 18:S1–S2.

Nishijyo T, Kawada A, Kanno T, Shiraiwa M, Takahara H. 1997. Isolation and molecular cloning of epidermal- and hair follicle-specific peptidylarginine deiminase (type III) from rat. J Biochem (Tokyo) 121:868–875.

Ohsawa T, Ishigami A, Akiyama K, Asaga H. 2001. Immunocytochemical localization of peptidylarginine deiminase type III, trichohyalin and deiminated trichohyalin in infant rat dorsal skin hair follicle. Biomed Res 22:91–97.

Rogers GE, Simmonds DH. 1958. Content of citrulline and other amino acids in a protein of hair follicles. Nature 182:186–187.

Rus'd AA, Ikejiri Y, Ono H, Yonekawa T, Shiraiwa M, Kawada A, Takahara H. 1999. Molecular cloning of cDNAs of mouse peptidylarginine deiminase type I, type III and type IV, and the expression pattern of type I in mouse. Eur J Biochem 259:660–669.

Senshu T, Sato T, Inoue T, Akiyama K, Asaga H. 1992. Detection of citrulline residues in deiminated proteins on polyvinylidene difluoride membrane. Anal Biochem 203:94–100.

Senshu T, Akiyama K, Kan S, Asaga H, Ishigami A, Manabe M. 1995. Detection of deiminated proteins in rat skin: probing with a monospecific antibody after modification of citrulline residues. J Invest Dermatol 105:163–169.

Senshu T, Akiyama K, Ishigami A, Nomura K. 1999. Studies on specificity of peptidylarginine deiminase reactions using an immunochemical probe that recognizes an enzymatically deiminated partial sequence of mouse keratin K1. J Dermatol Sci 21:113–126.

Smith MA. 1998. Alzheimer disease. Int Rev Neurobiol 42:1–54.

Tarcsa E, Marekov LN, Mei G, Melino G, Lee S-C, Steinert PM. 1996. Protein unfolding by peptidylarginine deiminase. Substrate specificity and structural relationships of the natural substrates trichohyalin and filaggrin. J Biol Chem 271:30709–30716.

Terakawa H, Takahara H, Sugawara K. 1991. Three types of mouse peptidylarginine deiminase: characterization and tissue distribution. J Biochem (Tokyo) 110:661–666.

Tian J, Shi J, Bailey K, Mann DM. 2004. Relationships between arteriosclerosis, cerebral amyloid angiopathy and myelin loss from cerebral cortical white matter in Alzheimer's disease. Neuropathol Appl Neurobiol 30:46–56.

Toda T, Kaji K, Kimura N. 1998. TMIG-2DPAGE: a new concept of two-dimensional gel protein database for research on aging. Electrophoresis 19:344–348.

Towbin H, Staehelin T, Gordon J. 1979. Electrophoretic transfer of proteins from polyacrylamide gels to nitrocellulose sheets: procedure and some applications. Proc Natl Acad Sci U S A 76:4350–4354.

Tsuchida M, Takahara H, Minami N, Arai T, Kobayashi Y, Tsujimoto H, Fukazawa C, Sugawara K. 1993. cDNA nucleotide sequence and primary structure of mouse uterine peptidylarginine deiminase. Detection of a 3′-untranslated nucleotide sequence common to the mRNA of transiently expressed genes and rapid turnover of this enzyme's mRNA in the estrous cycle. Eur J Biochem 215:677–685.

Vincent SR, Leung E, Watanabe K. 1992. Immunohistochemical localization of peptidylarginine deiminase in the rat brain. J Chem Neuroanat 5:159–168.

Watanabe K, Senshu T. 1989. Isolation and characterization of cDNA clones encoding rat skeletal muscle peptidylarginine deiminase. J Biol Chem 264:15255–15260.

Watanabe K, Akiyama K, Hikichi K, Ohtsuka R, Okuyama A, Senshu T. 1988. Combined biochemical and immunochemical comparison of peptidylarginine deiminases present in various tissues. Biochim Biophys Acta 966:375–383.

Acta Neuropathol (2005) 109: 353–366
DOI 10.1007/s00401-004-0966-4

REGULAR PAPER

Kuniaki Tsuchiya · Shigeo Murayama · Kazuko Mitani
Tatsuro Oda · Kunimasa Arima · Masaru Mimura
Hiroshi Nagura · Chie Haga · Haruhiko Akiyama
Hiroshi Yamanouchi · Hidehiro Mizusawa

Constant and severe involvement of Betz cells in corticobasal degeneration is not consistent with pyramidal signs: a clinicopathological study of ten autopsy cases

Received: 13 September 2004 / Revised: 15 November 2004 / Accepted: 16 November 2004 / Published online: 25 February 2005

Abstract This report concerns a clinicopathological study of three additional patients with corticobasal degeneration (CBD), described here for the first time, and a clinicopathological correlation between pyramidal signs and upper motor neuron involvement, in ten autopsy cases of CBD, including seven cases reported by us previously. We investigated pyramidal signs, including hyperreflexia, Babinski sign, and spasticity, and involvement of the primary motor cortex and pyramidal tract, focusing on the astrocytosis of the fifth layer of the primary motor cortex. Pyramidal signs were observed in six (60%) of the ten cases. Hyperreflexia was evident in six patients (60%), with spasticity being observed in three patients (30%). Loss of Betz cells associated with prominent astrocytosis and presence of ballooned neurons in the fifth layer of the primary motor cortex was observed in all ten cases. In all cases, involvement of the pyramidal tract was obvious in the medulla oblongata, without involvement of the pyramidal tract in the midbrain. Constant and severe involvement of the fifth layer of the primary motor cortex, including the Betz cells, has not previously been reported in CBD. We suggest that the pyramidal signs in CBD have been disregarded.

Keywords Betz cells · Charcot-Rebeiz disease · Corticobasal degeneration · Pyramidal signs · Pyramidal tract degeneration

K. Tsuchiya (✉)
Department of Laboratory Medicine and Pathology,
Tokyo Metropolitan Matsuzawa Hospital, 2-1-1,
Kamikitazawa, Setagaya-ku, 156-0057 Tokyo, Japan
E-mail: ktsuchi@jcom.home.ne.jp
Tel.: +81-3-33037211
Fax: +81-3-33045109

K. Tsuchiya · C. Haga · H. Akiyama
Department of Neuropathology,
Tokyo Institute of Psychiatry, Tokyo, Japan

K. Tsuchiya · H. Mizusawa
Department of Neurology,
Tokyo Medical and Dental University, Tokyo, Japan

S. Murayama
Department of Neuropathology,
Tokyo Metropolitan Gerontology, Tokyo, Japan

K. Mitani · H. Nagura · H. Yamanouchi
Department of Neurology,
Tokyo Metropolitan Geriatric Hospital, Tokyo, Japan

T. Oda
Department of Psychiatry, National Shimofusa Sanatorium,
Chiba, Japan

K. Arima
Department of Laboratory Medicine,
National Center Hospital for Mental,
Nervous and Muscular Disorders, Tokyo, Japan

M. Mimura
Department of Neuropsychiatry,
Showa University School of Medicine, Tokyo, Japan

Introduction

Corticobasal degeneration (CBD) [3, 9, 10, 11, 16, 17, 20, 21, 28, 29, 31, 38, 42, 43, 51, 56, 58, 59, 72, 73, 74] or cortical-basal ganglionic degeneration [4, 5, 37] was first described by Rebeiz et al. in 1967 and 1968 [52, 53] as corticodentatonigral degeneration with neuronal achromasia. It is a rare neurodegenerative disorder and can be classified as "Parkinson plus" together with multiple system atrophy and progressive supranuclear palsy [22, 23, 24, 25, 30]. CBD may occur more frequently as initially thought, as indicated by the growing number of reported cases since the report of three autopsy cases of CBD by Gibb et al. [18] in 1989. With

more autopsy cases and clinicopathological studies of CBD, Goetz [19] in 2000 noticed that the CBD prototype may be the "atypical Parkinson's disease" described by Jean-Martin Charcot. In 2000, Agid [1] proposed that the clinical diagnosis of CBD was evident when the following features were observed in a given patient: an akineto-rigid syndrome unresponsive to L-DOPA associated with dystonic postures, apraxia, and a marked asymmetry of symptoms. Furthermore, Agid noted that if Jean-Martin Charcot was really the first to point out this form of parkinsonism (atypical Parkinson's disease) at the end of the last century, that is, 75 years before Rebeiz et al. described the three cases that became the archetype of the syndrome, it might perhaps be more reasonable to name this affliction Charcot-Rebeiz disease, at least until its mechanism and causes are discovered. In 1999, Tsuchiya et al. [65] found that basal ganglia lesions of Group B Pick's disease, which have prominent degeneration of the pallidum and substantia nigra, and those classified by Constantinidis et al. [8] in 1974 and Constantinidis [7] in 1985, which macroscopically show frontal atrophy and histologically cortical degeneration characterized by ballooned neurons without Pick bodies, are fundamentally consistent with the basal ganglia lesions of CBD elucidated by Tsuchiya et al. in 1997 [63]. Recently, CBD has been regarded a member of the "Pick complex" [13, 60], a "unifying concept of overlapping clinical syndromes and neuropathological findings of neurodegenerative diseases causing focal cortical atrophy", as proposed by Kertesz and Munoz, emphasizing the similarities, rather than the differences, between them [32, 33, 44].

It is generally believed that pyramidal signs, including hyperreflexia, Babinski sign, and spasticity, are usually observed in cases of CBD [6, 36, 54, 55, 76]. Furthermore, it has been reported that the frequency of pyramidal signs in cases of CBD, ranged from extremely common [37] to about 27% [57]. In contrast, clinicopathological correlation studies of pyramidal signs with the lesions of the primary motor cortex and pyramidal tract in CBD have been rare [27, 53].

The purpose of this report is to describe the clinicopathological features of CBD in ten Japanese autopsy cases, including pyramidal signs and involvement of the primary motor cortex and pyramidal tract, focusing on the presence or absence of astrocytosis in the fifth layer of the primary motor cortex associated with presence of ballooned neurons and loss of Betz cells; i.e., small groupings of fat granule cells in the spaces in which Betz cells were present [66, 70]. We investigated the clinicopathological correlation between pyramidal signs and involvement of the pyramidal tract in ten autopsy cases. In addition, we address in the discussion the pathological heterogeneity in the primary motor cortex among multiple system atrophy (MSA), amyotrophic lateral sclerosis (ALS) with dementia, and CBD, paying attention to the clinicopathological dissociation of the pyramidal signs and lesions of the Betz cells and pyramidal tract in CBD, compared with those of MSA and ALS with dementia.

Materials and methods

The present investigation was carried out on ten autopsy cases from three Japanese institutions. The clinical records and tissue specimens in cases 1, 3, 6, 7, 8, and 9 were from the Department of Neuropathology, Tokyo Institute of Psychiatry. Those in cases 2, 5, and 10 were from the Department of Neuropathology, Tokyo Metropolitan Gerontology, and those in case 4 were from the Department of Laboratory Medicine, National Center Hospital for Mental, Nervous, and Muscular Disorders.

After fixation in formalin, the brains of the ten cases were sectioned in the coronal plane. The cerebral hemisphere and/or small blocks, including the frontal, temporal, parietal, and occipital lobes, and the striatum, pallidum, subthalamic nucleus, thalamus, amygdala, and hippocampus, were taken. Additional tissue blocks were taken from the midbrain, including the substantia nigra, brain stem, and cerebellum. The brains were embedded in paraffin and cut at a thickness of about 10 μm. The sections were stained with hematoxylin-eosin (HE), and also using the Klüver-Barrera, Holzer, Bodian, methenamine silver, and modified Gallyas-Braak methods. Immunocytochemistry was performed using antibodies against human-tau pool 2 (from Dr. H. Mori; Osaka City university), polyclonal neurofilament (200 kDa), and glial fibrillary acidic protein (GFAP).

The neuropathological diagnosis in the ten cases was made on the basis of the findings described below, which included many astrocytic plaques and ballooned neurons [14, 15, 34, 35] in the cerebral cortex and the widespread presence of argyrophilic threads in the central nervous system (Figs. 1, 2, 3). The neuropathological features of all ten cases were fundamentally consistent with the recently proposed neuropathological criteria for CBD by Dickson et al. [12].

The clinicopathological findings in cases 1, 3, 4, 6, 7, 8, and 9 have been reported previously by Tsuchiya et al. [61], Mimura et al. [39], Arima et al. [2], Oda et al. [49], Mitani et al. [40], Miyazaki et al. [41], and Oda et al. [50], respectively. The neuropathological hallmarks of case 7, including the abnormal cytoskeletal pathology peculiar to CBD, have been described by Uchihara et al. [71]. The distribution of cerebral cortical lesions identified by light microscopy, classified into three categories in cases 1, 6, 7, 8, and 9, has been reported by Tsuchiya et al. [62]. The distribution of basal ganglia lesions, classified into three categories in cases 1, 4, 6, 7, 8, and 9, has been investigated by Tsuchiya et al. [63]. Serial brain CT of cases 1 and 8 have also been described by Tsuchiya et al. [64].

Basal ganglia lesions, including the pallidum, caudate nucleus, putamen, and subthalamic nucleus, was

Table 1 Summary of clinical and pathological features (*M* male, *F* female, + presence, − absence,*severe* severe neuronal loss, *moderate*moderate neuronal loss, *slight* slight neuronal loss,*PD* Pick's disease, *CBD* corticobasal degeneration, *PSP* progressive supranuclear palsy)

Case	1	2	3	4	5	6	7	8	9	10
Clinical diagnosis	CBD	CBD	PD or frontal lobe dementia	PD	CBD	PSP	CBD	PD	PD	Atypical PSP
Heredity	−	−	−	−	−	−	−	−	−	−
Sex	M	M	F	M	M	F	M	F	F	F
Age at onset (years)	65	71	62	64	64	45	63	58	62	67
Duration ofthe disease	2 years 1 month	4 years 8 months	2 years 9 months	9 years 2 months	5 years 8 months	8 years	3 years 10 months	3 years 7 months	7 years	11 years
Initial sign	Limbkinetic apraxia	Limbkinetic apraxia	Motor aphasia	Aphasia	Memory disturbance	Delusion of persecution	Limbkinetic apraxia	Abnormal behavior	Abnormal behavior	Memory disturbance
Muscular rigidity	+	+	−	+	+	+	+	−	+	+
Dementia	+	+	+	+	+	+	+	+	+	+
Brain weight (g)	1,370	1,345	1,200	1,120	1,100	1,050	1,040	987	940	810
Cerebral cortex										
Neuronal loss	+	+	+	+	+	+	+	+	+	+
Ballooned neurons	+	+	+	+	+	+	+	+	+	+
Astrocytic plaques	+	+	+	+	+	+	+	+	+	+
Pallidum	Severe	Severe	Severe	Severe	Severe	Severe	Severe	Severe	Severe	Severe
Striatum (caudate nucleus and putamen)	Moderate	Moderate	Moderate	Moderate	Moderate	Moderate	Moderate	Moderate	Moderate	Moderate
Subthalamic nucleus	Slight	Slight	Slight	Slight	Slight	Slight	Slight	Slight	Slight	Slight
Neuronal loss in the Substantia nigra	+	+	+	+	+	+	+	+	+	+
References	[61, 62, 63, 64]		[39]	[2, 63]		[49, 62, 63]	[40, 62, 63, 71]	[41, 62, 63, 64]	[50, 62, 63]	

Table 2 Clinicopathological correlation between pyramidal signs and involvement of the primary motor cortex and pyramidal tract (+ present, – absent, *N.R.* not recorded)

Case	1	2	3	4	5	6	7	8	9	10
Pyramidal sign	+	+	N.R.	–	–	+	+	–	+	+
Hyperreflexia	+	+	N.R.	–	–	+	+	–	+	+
Babinski sign	+	–	N.R.	–	–	–	–	–	N.R.	–
Spasticity	+	+	N.R.	N.R.	–	N.R.	+	–	N.R.	N.R.
Loss of Betz cells	+	+	+	+	+	+	+	+	+	+
Astrocytosis of the primary motor cortex layer V	+	+	+	+	+	+	+	+	+	+
Degeneration of the pyramidal tract										
Midbrain	–	–	–	–	–	–	–	–	–	–
Medulla oblongata	+	+	+	+	+	+	+	+	+	+

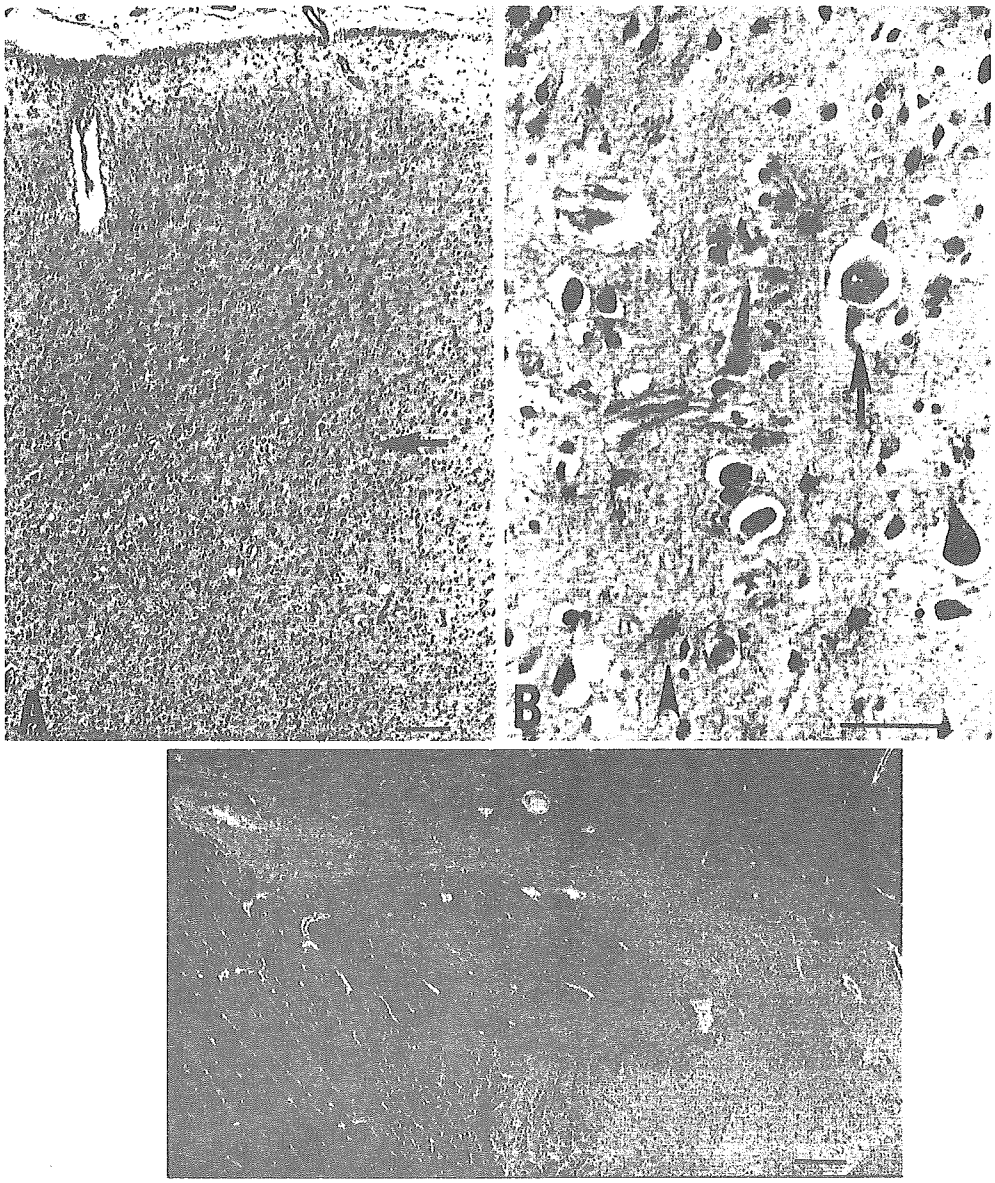

Fig. 1 **A–C** Case 2. **A** Superior frontal gyrus showing obvious neuronal loss. **B**. Enlargement of area indicated by *arrow* in **A** showing a ballooned neuron (*arrow*) and fibrillary glia (*arrowhead*). **C** Relative preservation of the subthalamic nucleus (*arrow*). **A, B** HE stain; **C** Klüver-Barrera stain; *bars* **A** 0.2 mm, **B** 0.05 mm, **C** 0.5 mm

classified as follows. Lesions identified by light microscopy were assigned to one of three categories: slight, showing relative preservation of the neurons with slight proliferation of the glia; moderate, showing obvious neuronal loss with evident astrocytosis and slight fibrillary gliosis; or severe, showing pronounced neuronal loss with neuropil rarefaction and/or prominent fibrillary gliosis. The classification of basal ganglia lesions described above is fundamentally consistent with the classification of basal ganglia lesions in CBD,

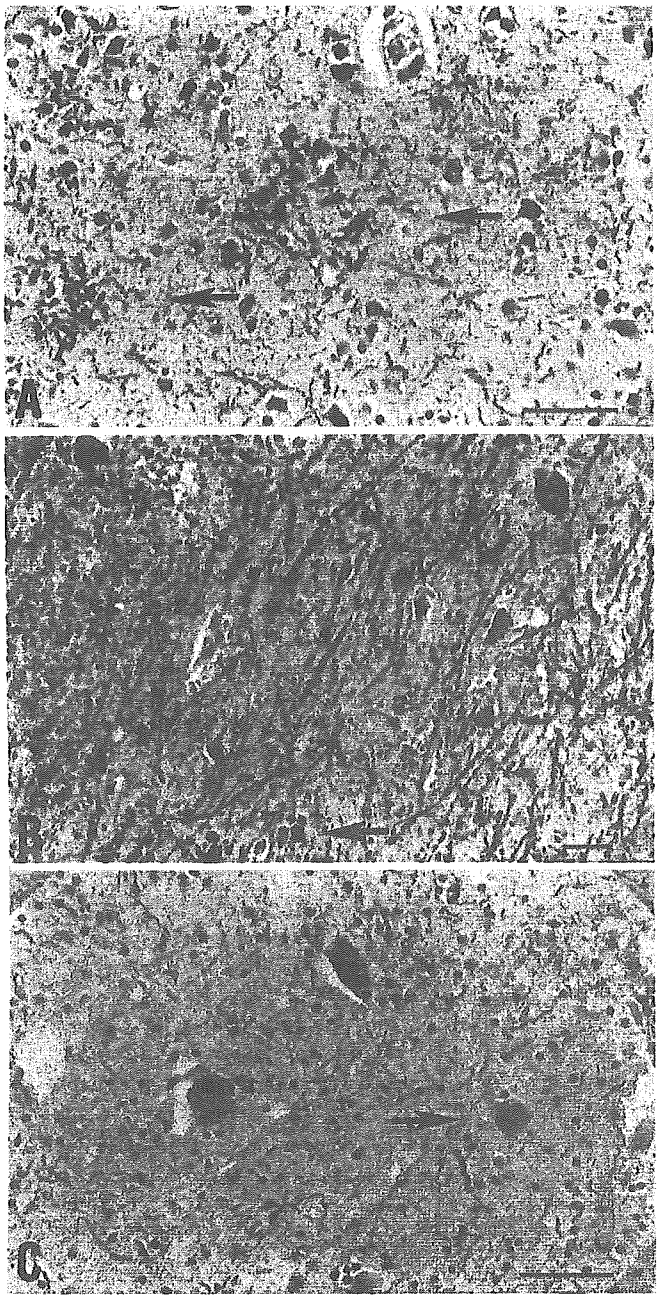

Fig. 2 A–C Case 5. **A** Astrocytic plaque (*arrow*) in the cerebral cortex. **B** Substantia nigra showing prominent neuronal loss with free melanin (*arrow*). **C** Substantia nigra showing neurofibrillary tangles (*arrow*). **A** modified Gallyas-Braak stain, **B** Klüver-Barrera stain, **C** modified Gallyas-Braak stain; *bars* **A–C** 0.05 mm

Pick's disease with Pick bodies (PDPB) [65], a generalized variant of Pick's disease (gvPD) [67], diffuse neurofibrillary tangles (NFT) with calcification, reported by Tsuchiya et al. [63, 65, 67, 69], respectively. The clinical and pathological features of all cases are summarized in Table 1.

Pyramidal signs were judged to be present in patients who showed one or more signs of hyperreflexia in the extremities, Babinski sign, and spasticity in the extremities. Loss of Betz cells was judged to be present in cases that showed small groupings of lipofuscin-laden macrophages in the holes, from which Betz cells had presumably disappeared, in the primary motor cortex with the presence of normal and degenerated Betz cells in the absence of an internal granular layer [26, 45, 46, 47, 48, 75] (Fig. 4). Astrocytosis of primary motor cortex layer V was considered present in cases showing definite astrocytosis determined using HE and Holzer staining or immunohistochemistry using an antibody against GFAP (Fig. 4). Pyramidal tract degeneration was also judged as present in cases showing definite loss of myelinated fibers shown by Klüver-Barrera stain, accompanied by gliosis revealed using Holzer stain and immunohistochemistry using an antibody against GFAP (Fig. 5). The determination of loss of Betz cells, astrocytosis of primary motor cortex layer V, and the pyramidal tract degeneration described above was fundamentally consistent with that in MSA and ALS with dementia, as described by Tsuchiya et al. [66, 70]. The pertinent data are summarized in Table 2.

Case reports

Clinical course and neuropathological findings in case 2

The patient was a Japanese man aged 76 years at the time of death. He was in good health until the age of 71, when he became aware of clumsiness of the right hand and action tremor of the right upper extremity, followed by bradykinesia 3 months later and action tremor of the left upper extremity 7 months after the onset of the disease. A neurological examination at the age of 72 years (8 months after the disease onset), revealed right limbkinetic apraxia, mild agraphia, bilateral action myoclonus on the upper extremities, prominent on the right, muscular rigidity, bradykinesia, and hyperreflexia in the upper and lower extremities without Babinski sign. At this stage, obvious dementia was not observed. Neurological examination 1 year after disease onset disclosed evident dementia. At 2 years after the disease onset, he could no longer walk without assistance. Vertical ocular movement involvement and dysphagia were noticed 3 years after disease onset. During this period, he was bed-ridden. At 3 years 10 months after disease onset, severe dementia and spasticity were obvious. He died of pneumonia at age 76, 4 years 8 months after the onset of the disease. He was clinically diagnosed as having CBD.

The brain weighed 1,345 g. Macroscopic examination revealed atrophy of the posterior portion in the superior frontal gyrus abutting the precentral gyrus, atrophy of the pallidum, and depigmentation of the substantia nigra. A histological examination showed neuronal loss with astrocytosis, status spongiosus, many ballooned neurons, and astrocytic plaques in the cerebral cortex of the frontal and parietal lobes (Fig. 1A, B). In the primary mortor cortex layer V, there was loss of Betz cells associated with prominent astrocytosis and ballooned

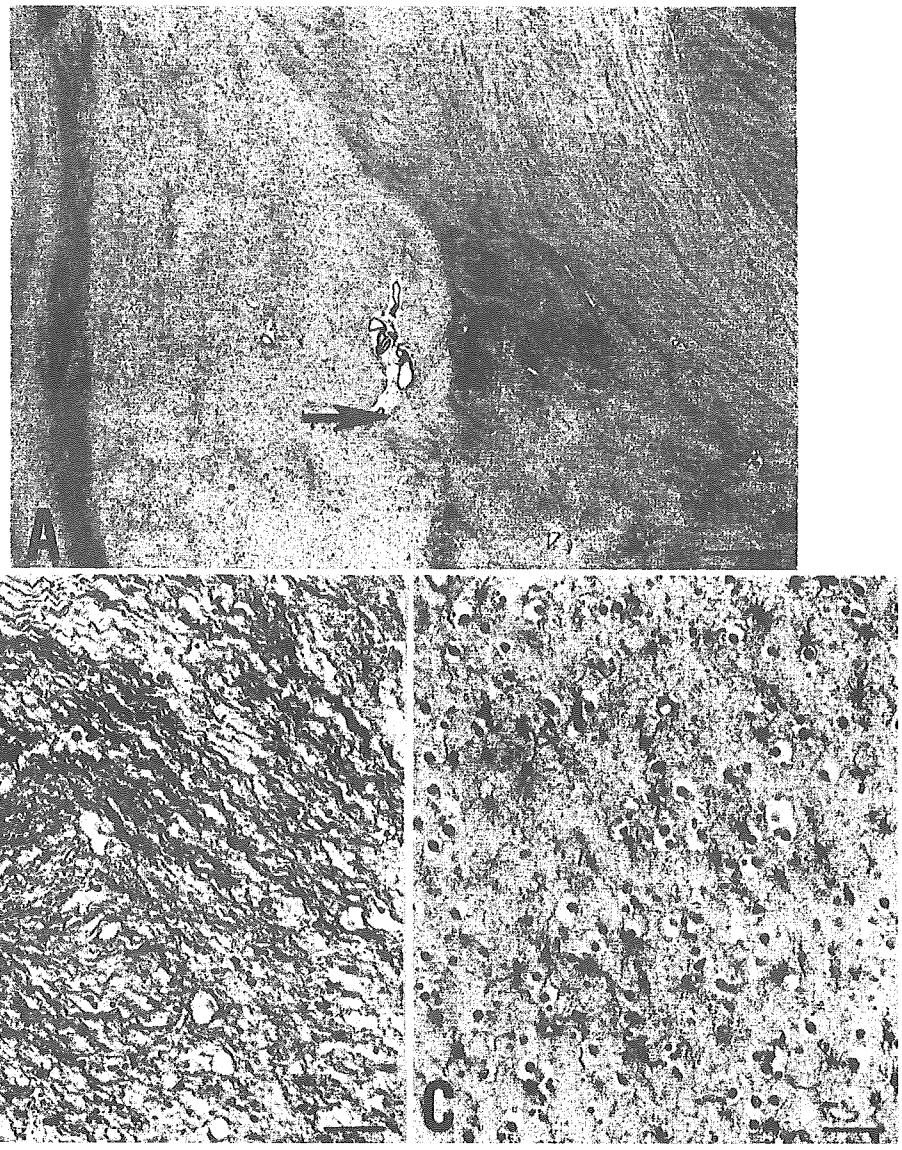

Fig. 3 **A–C** Case 10. **A** Obvious fibrillary gliosis in the pallidum (*arrow*), in contrast to slight fibrillary gliosis in the putamen. **B** Obvious fibrillary gliosis in the pallidum. **C** Slight fibrillary gliosis in the putamen. **A**, **B**, **C** Holzer stain; *bar*s **A** 1 mm; **B**, **C** 0.05 mm

neurons were present. Fibrillary gliosis was observed in the cerebral white matter. Neuronal loss was not observed in the hippocampus, parahippocampal gyrus, amygdala, nucleus basalis of Meynert, oculomotor nucleus, pontine nucleus, Purkinje cells, hypoglossal nucleus, dorsal motor nucleus of the vagus, or inferior olive. Severe neuronal loss was observed in the pallidum, prominently in the dorsal part. The caudate nucleus and putamen showed moderate neuronal loss, but the subthalamic nucleus disclosed relative preservation of the neurons with slight proliferation of the glia (Fig. 1C). In the substantia nigra, there was prominent neuronal loss with melanin pigment incontinence. In the dentate nucleus, there was mild neuronal loss and "grumose degeneration". Senile plaques were not observed using methenamine silver staining. Using modified Gallyas-Braak methods, a few NFT in the hippocampus CA1 and a small quantity of NFT in the parahippocampal gyrus were seen, compatible with stage II of Braak's classification, and many argyrophilic threads were encounterd in the central nervous system.

Clinical course and neuropathological findings in case 5

This autopsy case was a Japanese man who was 70 years old at the time of death. He was well until the age of 64, when he developed memory disturbance, followed by topographical disorientation 10 months later and aspontaneity 1 year 6 months after the onset of the disease. A neurological examination when the patient was 69 years old (4 years 4 months after the disease onset) revealed severe dementia (revised Hasegawa dementia rating scale 0), vertical ocular movement involvement, rigidity of the right upper and lower extremities, absence of Babinski sign and hyperreflexia in the upper and lower extremities. At 4 years 7 months after disease onset, he

could walk and eat a meal with assistance, but he was doubly incontinent. Dysphagia became evident 5 years 2 months after the onset of the disease. Severe dysphagia very often caused misswallowing, which necessitated a gastrostomy, performed 5 years 5 months after the disease onset. He died of repeated pneumonia, probably due to severe dysphagia, 5 years 8 months after the onset of the disease. He was clinically diagnosed as having CBD, mainly because of prominent dementia and obvious rigidity in the clinical stage without difficulty in walking, by one of the authors (K. Tsuchiya).

Fig. 4 Involvement of the primary motor cortex. **A**, **B** Case 1; **C**, **D** case 3; **E–G** case 7; **H**, **I** case 10. **A** Ballooned neuron (*large arrow*) and hypertrophic glia (*arrowhead*) in the primary motor cortex, including Betz cell (*small arrow*). **B** Loss of Betz cell (*large arrow*) in the primary motor cortex, including Betz cell (*small arrow*). **C** Ballooned neuron (*arrow*) in the primary motor cortex. **D** Loss of Betz cell (*large arrow*) in the primary motor cortex, including Betz cell (*small arrow*). **E** Obvious involvement of the primary motor cortex, including degenerated Betz cell (*arrow*), showing prominent spongy state in the upper cortical layers. **F** Enlargement of the area indicated by *arrow* in **E**, showing degenerated Betz cell (*arrow*) and hypertrophic glia (*arrowhead*). **G** Hypertrophic glia (*arrowhead*) in the primary motor cortex, including degenerated Betz cell (*arrow*). **H** Deep layer of the primary motor cortex, including Betz cell (*arrow*). **I** Enlargement of the area indicated by *arrow* in **H**, showing loss of Betz cell (*arrow*) and hypertrophic glia (*arrowhead*). **A**, **B**, **E**, **F**, **H**, **I** H.E. stain; **C**, **D** K-B stain; **G** Holzer stain; *bars* **A–D**, **F**, **G**, **I** 0.04 mm; **E**, **H** 0.2 mm

The brain weighed 1,100 g before fixation. Macroscopic examination revealed atrophy of the frontal and parietal lobes, with depigmentation of the substantia nigra. A histological examination showed neuronal loss with astrocytosis, status spongiosus, many ballooned neurons, and astrocytic plaques in the cerebral cortex of the frontal and parietal lobes (Fig. 2A). In the primary morter cortex layer V, there was loss of Betz cells associated with obvious astrocytosis and presence of ballooned neurons. In the cerebral white matter, hyalinosis of the small vessels was obvious. Neuronal loss was not observed in the hippocampus, parahippocampal gyrus, amygdala, pontine nucleus, Purkinje cells, hypoglossal nucleus, dorsal motor nucleus of the vagus, or inferior olive. Severe neuronal loss was encountered in the pallidum, prominently in the dorsal part. The caudate nucleus and putamen showed moderate neuronal loss, but the subthalamic nucleus disclosed relative preservation of the neurons with slight proliferation of the glia. In the substantia nigra, there was prominent neuronal loss with leakage of melanin pigment and the presence of NFT (Fig. 2B, C). In the dentate nucleus, there was mild neuronal loss and grumose degeneration. Senile plaques were not observed using methenamine silver staining. Using modified Gallyas-Braak staining, a few NFT in the hippocampus CA1 and a small quantity of NFT in the parahippocampal gyrus were seen, con-

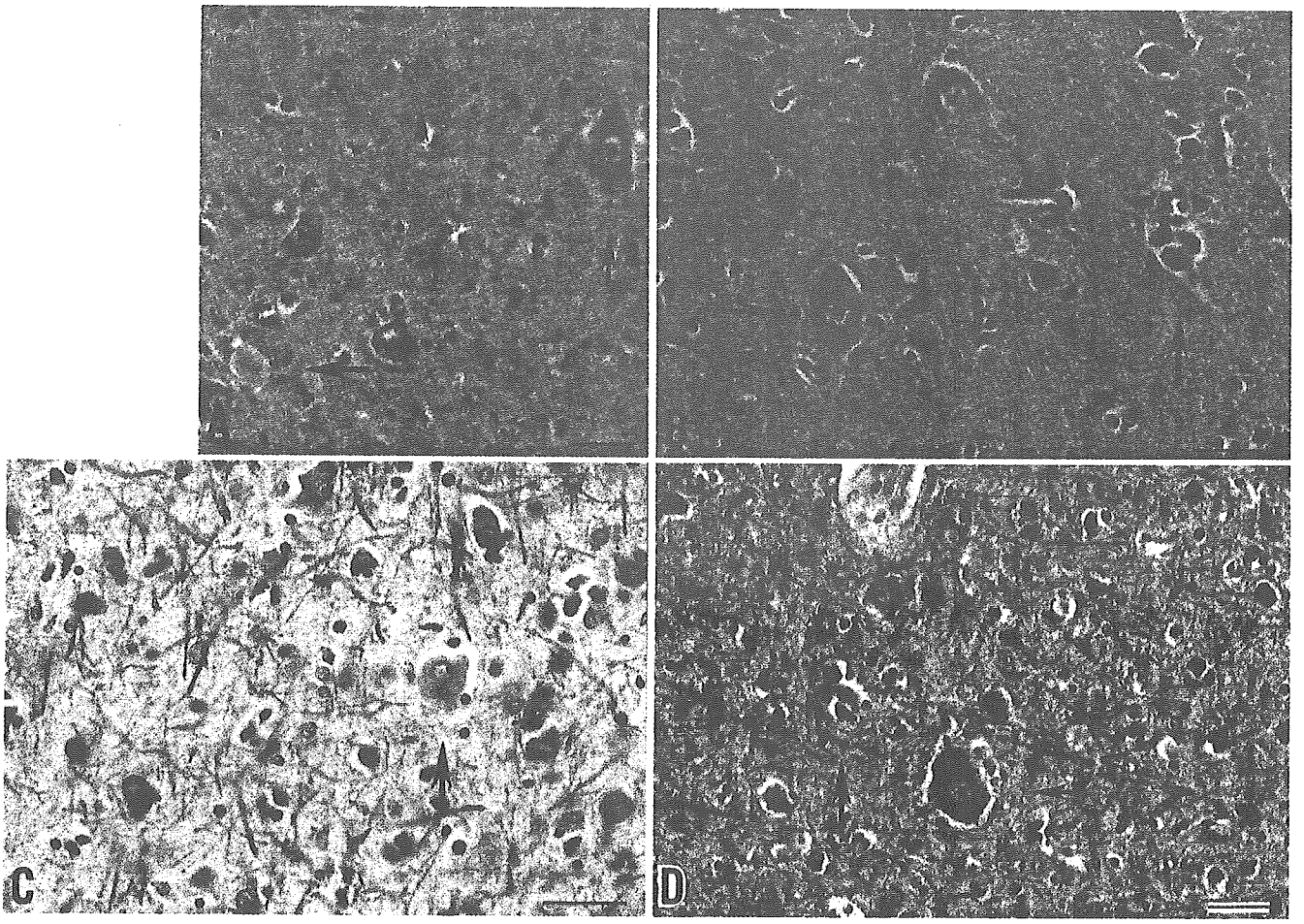

Fig. 4 (Contd.)

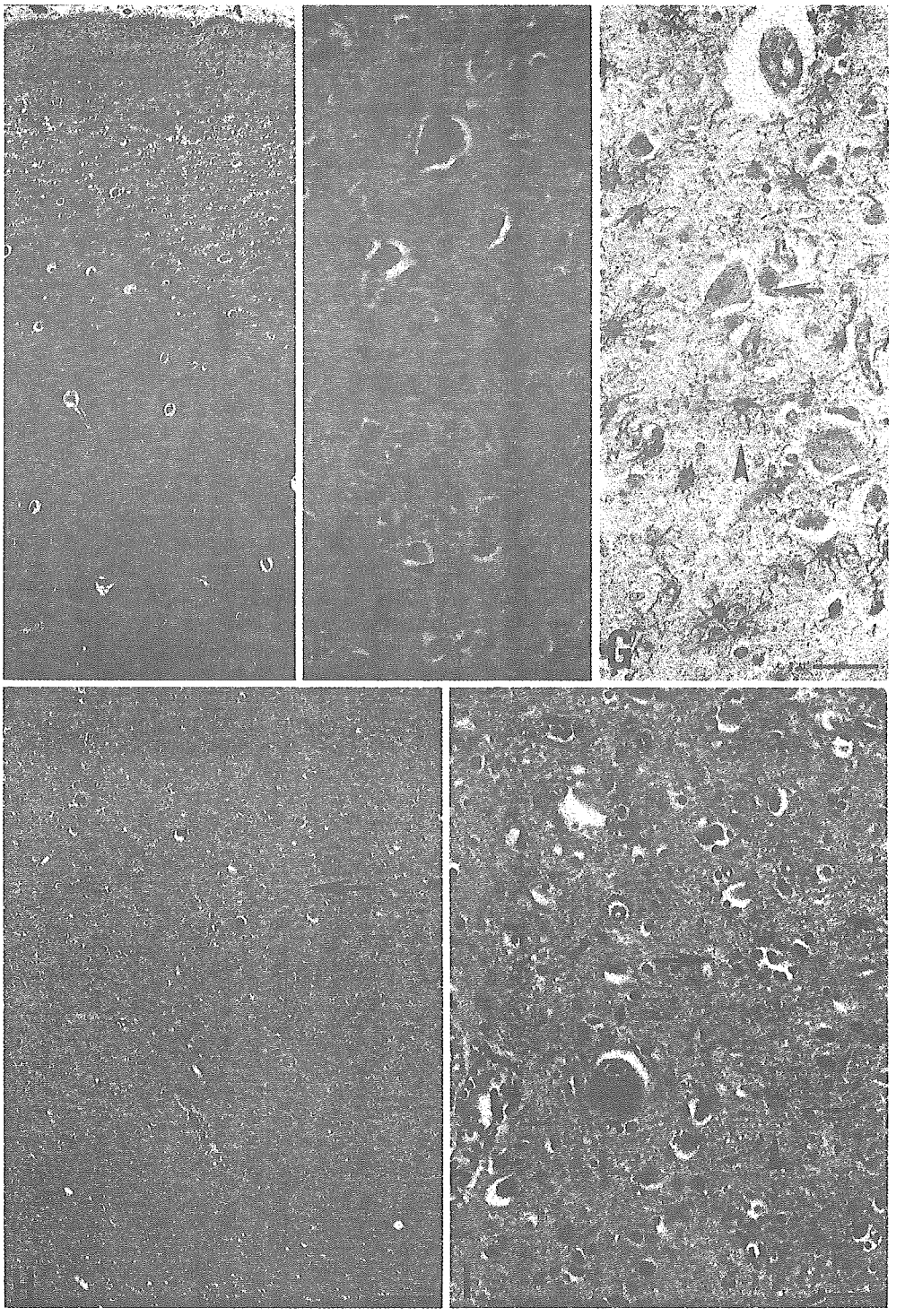

sistent with stage II of Braak's classification, as well as many argyrophic threads.

Clinical course and neuropathological findings in case 10

This patient was a Japanese woman aged 78 years at the time of death. She was in good health until the age of 67, when she developed memory disturbance, followed about 2 year later by action tremor, and at 3 years after the onset of the disease by difficulty in walking. At 5 years after the disease onset, memory disturbance worsened, followed by dyskinesia in the upper extremities. A neurological examination at the age of 75, 8 years after the disease onset, disclosed severe dementia, dyskinesia in the upper and lower extremities, hyperreflexia in the four extremities without Babinski sign. She died of

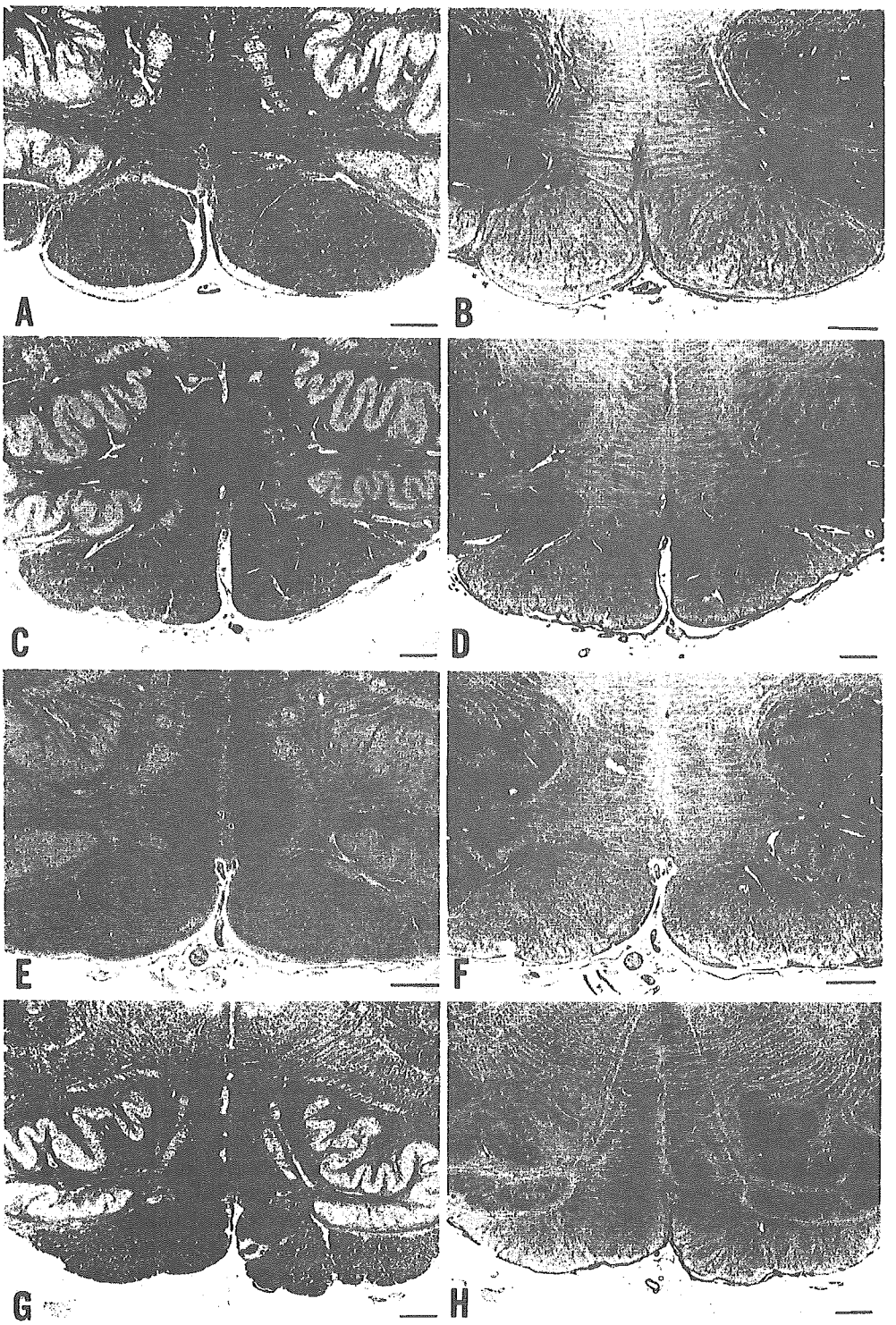

Fig. 5 A–H Involvement of the pyramidal tract in the medulla oblongata. **A, B** Case 1; **C, D** case 6; **E, F** case 7; **G, H** case 8. **A, C, E, G** Klüver-Barrera stain; **B, D, F, H** Holzer stain; *bars* **A–H** 1 mm

pneumonia at age 78, 11 years after the onset of the disease. She was clinically diagnosed as having atypical progressive supranuclear palsy.

The brain weighed 810 g. Macroscopic examination revealed atrophy of the frontal and parietal lobes, with depigmentation of the substantia nigra. A histological examination showed neuronal loss with astrocytosis, spongy state, many ballooned neurons, and astrocytic plaques in the cerebral cortex of the frontal and parietal lobes. In the primary motor cortex layer V, there was loss of Betz cells associated with prominent astrocytosis, and ballooned neurons were present. Fibrillary gliosis was observed in the cerebral white matter. Neuronal loss was not observed in the hippocampus, parahippocampal gyrus, amygdala, nucleus basalis of Meynert, oculomotor nucleus, trochlear nucleus, pontine nucleus, Purkinje

cells, hypoglossal nucleus, dorsal motor nucleus of the vagus, or inferior olive. Severe neuronal loss was observed in the pallidum, prominently in the dorsal part (Fig. 3A, B). The caudate nucleus and putamen (Fig. 3C) showed moderate neuronal loss, but the subthalamic nucleus disclosed relative preservation of the neurons with slight proliferation of the glia. In the substantia nigra, there was prominent neuronal loss with leakage of melanin pigment. In the dentate nucleus, there was mild neuronal loss and grumose degeneration. Senile plaques were not observed with methenamine silver staining. A few NFT in the hippocampus CA1 and a small quantity of NFT in the parahippocampal gyrus, compatible with stage II of Braak's classification, and many argyrophilic threads were encountered using modified Gallyas-Braak methods.

Results

Clinical features

The main clinical information on the ten patients (five males, five females) is summarized in Table 1. The patients had no hereditary burden. The age at onset of symptoms was from the fifth to eighth decade of life (average of 62 years 1 month). The duration of the disease ranged from 2 years 1 month in case 1 to 11 years in case 10 (mean duration 5 years 9 months). Three patients presented with limbkinetic apraxia as the initial sign (cases 1, 2, and 7). Two patients initially developed aphasia and motor aphasia (cases 3 and 4). Memory disturbance was observed in two patients as the initial sign (cases 5 and 10). Delusion of persecution was noted as the initial sign in case 6. Abnormal behavior, reminiscent of Pick's disease, was noticed as the initial sign in cases 8 and 9. Muscular rigidity was noted in eight patients during the clinical course, but in cases 3 and 8, with relative shorter clinical courses, muscular rigidity was not noticed. All ten cases presented with dementia during the clinical course.

Pathological features

The neuropathological data are also summarized in Table 1. Brain weights at autopsy ranged from 1,370 to 810 g (average 1,096.2 g). In the cerebral cortex of all ten cases, neuronal loss and gliosis associated with the presence of ballooned neurons and astrocytic plaques were encounterd in the frontal and parietal lobes. In all cases, the pallidum revealed severe neuronal loss and prominent gliosis, while moderate lesions were evident in the caudate nucleus and putamen. In the subthalamic nucleus, slight lesions were found in each CBD case examined in this study. Neuronal loss of the substantia nigra was prominent in all cases.

Clinicopathological correlation between pyramidal signs and involvement of the primary motor cortex and pyramidal tract

Pyramidal signs and involvement of the primary motor cortex and pyramidal tract are summarized in Table 2. Pyramidal signs, including hyperreflexia and Babinski sign, were noted in six cases (cases 1, 2, 6, 7, 9 and 10). Spasticity was noticed in only three cases (cases 1, 2, and 7). Loss of Betz cells was observed in all ten cases (Fig. 4). Furthermore, astrocytosis of the primary motor cortex layer V, detected by HE, Holzer, and GFAP staining, was obvious in all ten cases (Fig. 4). Degeneration of the pyramidal tract was found in each case, and the distal portion (medulla oblongata) was more affected than the proximal portion (midbrain), suggestive of a dying back phenomenon (Fig. 5).

Discussion

Clinical features

Pyramidal signs, including hyperreflexia, Babinski sign, and spasticity, are said to be common in CBD cases, but the frequency of pyramidal signs in CBD patients remains unclear to date. In 1990, Riley et al. [54], who designated CBD as cortical-basal ganglionic degeneration, described 15 patients with CBD, including 2 autopsy-confirmed CBD cases (patients 1 and 2 in their report), noticed that in their 15 patients, hyperreflexia associated with Babinski sign was observed in 5 patients (33%), but that hyperreflexia without Babinski sign was found in 7 patients (47%). Rinne et al. [55], in 1994, conducted a clinical study of 36 CBD cases, including 6 pathologically confirmed CBD cases, noted that hyperreflexia was observed in 26 patients (72%), with Babinski sign in 17 patients (47%). In 1997, Schneider et al. [57], who investigated clinical and neuropathological heterogeneity in 11 cases of pathologically diagnosed CBD, observed that 3 patients manifested Babinski sign (27%). Kompoliti et al. [36], in 1998, who examined the clinical presentation and pharmacological therapy in 147 CBD patients, including 7 autopsy-proven CBD cases, noted that pyramidal signs were observed in 84 CBD patients (57%), but that they were encountered in 6 cases (86%) of the 7 autopsy-proven CBD cases. In 1998, Wenning et al. [76] analyzed the natural history and survival of 14 patients with CBD confirmed at postmortem examination, and noticed that hyperreflexia was observed in 5 cases (36%), with Babinski sign being found in 3 cases (21%), about 3 years after the disease onset, but that hyperreflexia was observed in 7 cases (58%), with Babinski sign being found in 5 cases (42%), respectively, about 6.1 years after the disease onset. Boeve et al. [6], in 1999, investigated the pathological heterogeneity in 13 clinically diagnosed CBD patients and found 7 autopsy CBD cases among

these patients. Furthermore, Boeve et al. noted that in their 7 autopsy CBD cases, pyramidal signs were obvious in 4 cases (57%).

Reviewing the literature regarding the frequency of the pyramidal signs in CBD, including hyperreflexia, Babinski sign, and spasticity, it becomes clear that there are many discrepancies between the frequencies of the pyramidal signs in CBD cases reported to date.

Pathological features

Neuropathological studies of CBD, focusing on the primary motor cortex and pyramidal tract, are very rare. Rebeitz et al. [53] noticed that in their three autopsy cases, in which case 1 had a very brisk left patellar reflex with cases 2 and 3 having prominent Babinski sign, there was evident pyramidal tract involvement in cases 2 and 3, but that in case 1 the Betz cells in the precentral cortex appeared normal with a good complement of Nissl granules. Gibb et al. [18] described three autopsy cases of CBD, in which three cases clinically presented with brisk tendon reflexes, but Babinski sign was only encountered in case 2. In their pathological findings, Gibb et al. noted that their three cases had mild to moderate corticospinal tract involvement, but they did not notice whether or not there was loss of Betz cells. In contrast, Horoupian and Chu [27] reported an autopsy case of CBD, in which bilateral Babinski signs, more prominent on the right, were clinically observed, and the pathological examination revealed prominent neuronal loss of the primary motor cortex, including Betz cells, associated with astrocytosis and presence of ballooned neurons.

From the literature concerning the involvement of the primary motor cortex and pyramidal tract in CBD, it becomes obvious that there have been few reports showing loss of Betz cells in the primary motor cortex and involvement of the pyramidal tract of CBD patients. Thus, our data, showing constant and severe involvement of Betz cells associated with constant involvement of the pyramidal tract in the medulla oblongata in ten cases of CBD, are important.

Clinicopathological correlation and pathological heterogeneity in the primary motor cortex among MSA, ALS with dementia, and CBD

Tsuchiya et al. [66] investigated the pyramidal signs, including spasticity, hyperreflexia, and Babinski sign, and the involvement of the primary motor cortex and pyramidal tract, in seven Japanese autopsy cases of MSA. In that study, pyramidal signs were observed in six (86%) of the seven MSA autopsy cases. Hyperreflexia and Babinski sign were each evident in five patients, but spasticity was observed in only one patient. Loss of Betz cells and presence of glial cytoplasmic inclusions (Papp-Lantos inclusions) in the primary motor cortex were noticed in all seven MSA autopsy cases. Astrocytosis in the fifth layer of the primary motor cortex was noted in five (71%) of the seven MSA autopsy cases. Involvement of the pyramidal tract in the medulla oblongata was observed in all seven MSA autopsy cases, but no involvement of the pyramidal tract in the midbrain was evident in any of the six autopsy cases in which this structure was examined.

Subsequently, Tsuchiya et al. [70] explored the pyramidal signs, including hyperreflexia, Babinski sign, and spasticity, as well as the involvement of the primary motor cortex and pyramidal tract, in eight Japanese autopsy cases of ALS with dementia. Pyramidal signs were observed in seven (88%) of the eight autopsy cases. Hyperreflexia and Babinski sign were evident in seven (88%) and three (38%) patients, respectively, but spasticity was not observed in any of the eight patients. Loss of Betz cells in the primary cortex was evident in all seven autopsy cases in which this structure was examined. In contrast, astrocytosis in the fifth layer of the primary motor cortex was noticed in only three cases (38%). Involvement of the pyramidal tract in the medulla oblongata was observed in all eight ALS with dementia autopsy cases, but no involvement of the pyramidal tract in the midbrain was found in any of the eight autopsy cases.

Given the high frequency of pyramidal signs in MSA (86%) [66] and ALS with dementia (88%) [70], the relatively low frequency of pyramidal signs (60%) in the ten CBD autopsy cases seen in the present study deserves a mention.

In this study, constant and severe involvement of the primary motor cortex, including loss of Betz cells and obvious astrocytosis of the fifth layer of the primary motor cortex, was observed in all ten CBD cases, suggesting that in CBD there is a clinicopathological dissociation between the involvement of the primary motor cortex and pyramidal tract, and pyramidal signs. In contrast, in seven MSA autopsy cases reported by Tsuchiya et al., astrocytosis in the fifth layer of the primary motor cortex was noticed in five cases (71%), consistent with the high frequency of pyramidal signs (86%), and in eight ALS with dementia cases reported by Tsuchiya et al., astrocytosis in the fifth layer of the primary motor cortex was noted in only three cases (38%), inconsistent with the high frequency of the pyramidal signs (88%).

On the basis of our data showing that pyramidal sign were observed in six (60%) of the ten CBD autopsy cases, and that astrocytosis in the fifth layer of the primary motor cortex and loss of Betz cells were obvious in all ten CBD autopsy cases, we believe that the pyramidal signs in CBD have been disregarded.

Acknowledgements We wish to express our gratitude to former Prof. H. Tsukagoshi (Department of Neurology, Tokyo Medical and Dental University) for his valuable advice. We also wish to thank to Mr. Y. Shoda and Ms E. Matsui for their photographic assistance.

References

1. Agid Y (2000) Conclusions. Adv Neurol 82:241–244
2. Arima K, Uesugi H, Fujita I, Sakurai Y, Oyanagi S, Andoh S, Izumiyama Y, Inose T (1994) Corticonigral degeneration with neuronal achromasia presenting with primary progressive aphasia: ultrastructural and immunocytochemical studies. J Neurol Sci 127:186–197
3. Armstrong RA, Cairns NJ, Lantos PL (2000) A quantitative study of the pathological lesions in the neocortex and hippocampus of twelve patients with corticobasal degeneration. Exp Neurol 163:348–356
4. Bergeron C, Pollanen MS, Weyer L, Black SE, Lang AE (1996) Unusual clinical presentations of cortical-basal ganglionic degeneration. Ann Neurol 40:893–900
5. Bergeron C, Davis A, Lang AE (1998) Corticobasal ganglionic degeneration and progressive supranuclear palsy presenting with cognitive decline. Brain Pathol 8: 355-365
6. Boeve BF, Maraganore DM, Parisi JE, Ahlskog JE, Graff-Radford N, Caselli RJ, Dickson DW, Kokmen E, Petersen RC (1999) Pathologic heterogeneity in clinically diagnosed corticobasal degeneration. Neurology 53:795–800
7. Constantinidis J (1985) Pick dementia: anatomoclinical correlations and pathophysiological considerations. In: Rose FC (ed) Interdisciplinary topics in gerontology, vol 19. Karger, Basel, pp 72–97
8. Constantinidis J, Richard J, Tissot R (1974) Pick's disease. Histological and clinical correlations. Eur Neurol 11:208–217
9. Dickson DW (1999) Neuropathologic differentiation of progressive supranuclear palsy and corticobasal degeneration. J Neurol 246 [Suppl 2]:II/6–II/15
10. Dickson DW, Litvan I (2003) Corticobasal degeneration. In: Dickson DW (ed) Neurodegeneration: the molecular pathology of dementia and movement disorder. ISN Neuropath Press, Basel, pp 115–123
11. Dickson DW, Liu W-K, Ksiezak-Reding H, Yen S-H (2000) Neuropathologic and molecular considerations. Adv Neurol 82:9–27
12. Dickson DW, Bergeron C, Chin SS, Duyckaerts C, Horoupian D, Ikeda K, Jellinger K, Lantos PL, Lippa CF, Mirra SS, Tabaton M, Vonsattel JP, Wakabayashi K, Litvan I (2002) Office of rare diseases neuropathologic criteria for corticobasal degeneration. J Neuropathol Exp Neurol 61:935–946
13. Duyckaerts C, Hauw J-J (2000) Diagnostic controversies: another view. Adv Neurology 82:233–240
14. Feany MB, Dickson DW (1995) Widespread cytoskeletal pathology characterizes corticobasal degeneration. Am J Pathol 146:1388–1396
15. Feany MB, Mattiace LA, Dickson DW (1996) Neuropathologic overlap of progressive supranuclear palsy, Pick's disease and corticobasal degeneration. J Neuropathol Exp Neurol 55:53–67
16. Ferrer I, Hernández I, Boada M, Llorente A, Rey MJ, Cardozo A, Ezquerra M, Puig B (2003) Primary progressive aphasia as the initial manifestation of corticobasal degeneration and unusual tauopathies. Acta Neuropathol 106:419–435
17. Forman MS, Zhukareva V, Bergeron C, Chin S S-M, Grossman M, Clark C, Lee V M-Y, Trojanowski JQ (2002) Signature tau neuropathology in gray and white matter of corticobasal degeneration. Am J Pathol 160:2045–2053
18. Gibb WRG, Luthert PJ, Marsden CD (1989) Corticobasal degeneration. Brain 112:1171–1192
19. Goetz CG (2000) Nineteenth century studies of atypical parkinsonism: Charcot and his Salpêtrière school. Adv Neurology 82:1–8
20. Grimes DA, Lang AE, Bergeron CB (1999) Dementia as the most common presentation of cortical-basal ganglionic degeneration. Neurology 53:1969–1974
21. Hattori M, Hashizume Y, Yoshida M, Iwasaki I, Hishikawa N, Ueda R, Ojika K (2003) Distribution of astrocytic plaques in the corticobasal degeneration brain and comparison with tuft-shaped astrocytes in the progressive supranuclear palsy brain. Acta Neuropathol 106:143–149
22. Hauw J-J, Agid Y (2003) Progressive supranuclear palsy (PSP) or Steele-Richardson-Olszewski disease. In: Dickson DW (ed) Neurodegeneration: The molecular pathology of dementia and movements disorder. ISN Neuropath Press, Basel, pp 103–114
23. Hauw J-J, Verny M, Delaère P, Cervera P, He Y, Duyckaerts C (1990) Constant neurofibrillary changes in progressive supranuclear palsy. Basic differences with Alzheimer's disease and aging. Neurosci Lett 119:182–186
24. Hauw J-J, Daniel SE, Dickson D, Horoupian DS, Jellinger K, Lantos PL, McKee A, Tabaton M, Litvan I (1994) Preliminary NINDS neuropathologic criteria for Steele-Richardson-Olszewski syndrome (progressive supranuclear palsy). Neurology 44:2015-2019
25. Hauw J-J, Verny M, Ruberg M, Duyckaerts C (1998) The neuropathology of progressive supranuclear palsy (PSP) or Steele-Richardson-Olszewski disease. In: Markesbery WR (ed) Neuropathology of dementing disorders. Arnold, London, pp 193–218
26. Holmes G (1909) The pathology of amyotrophic lateral sclerosis. Rev Neurol Psychiatry 8:693–725
27. Horoupian DS, Chu PL (1994) Unusual case of corticobasal degeneration with tau/Gallyas-positive neuronal and glial tangles. Acta Neuropathol 88:592–598
28. Ikeda K, Akiyama H, Iritani S, Kase K, Arai T, Niizato K, Kuroki N, Kosaka K (1996) Corticobasal degeneration with primary progressive aphasia and accentuated cortical lesion in superior temporal gyrus: case report and review. Acta Neuropathol 92:534–539
29. Ikeda K, Akiyama H, Arai T, Tsuchiya K (2002) Pick-body-like inclusions in corticobasal degeneration differ from Pick bodies in Pick's disease. Acta Neuropathol 103:115–118
30. Jellinger KA, Bancher C (1992) Neuropathology. In: Litvan I, Agid Y (eds) Progressive supranuclear palsy. Clinical and research approaches. Oxford University Press, New York, pp 44–88
31. Katsuse O, Iseki E, Arai T, Akiyama H, Togo T, Uchikado H, Kato M, Silva R de, Lees A, Kosaka K (2003) 4-report tauopathy sharing pathological and biochemical features of corticobasal degeneration and progressive supranuclear palsy. Acta Neuropathol 106:251–260
32. Kertesz A (1998) Pick's disease and Pick complex: introductory nosology. In: Kertesz A, Munoz DG (eds), Pick's disease and Pick complex, Wiley-Liss, New York, pp 1–11
33. Kertesz A, Munoz DG (1998) Clinical and pathological overlap in Pick complex. In: Kertesz A, Munoz DG (eds) Pick's disease and Pick complex. Wiley-Liss, New York, pp 281–286
34. Komori T (1999) Tau-positive glial inclusions in progressive supranuclear palsy, corticobasal degeneration and Pick's disease. Brain Pathol 9:663–679
35. Komori T, Arai N, Oda M, Nakayama H, Mori H, Yagishita S, Takahashi T, Amano N, Murayama S, Murakami S, Shibata N, Kobayashi M, Sasaki S, Iwata M (1998) Astrocytic plaques and tufts of abnormal fibers do not coexist in corticobasal degeneration and progressive supranuclear palsy. Acta Neuropathol 96:401–408
36. Kompoliti K, Goetz CG, Boeve BF, Maraganore DM, Ahlskog JE, Marsden CD, Bhatia KP, Greene PE, Przedborski S, Seal EC, Burns RS, Hauser RA, Gauger LL, Factor SA, Molho ES, Riley DE (1998) Clinical presentation and pharmacological therapy in corticobasal degeneration. Arch Neurol 55:957–961
37. Lang AE, Riley DE, Bergeron C (1994) Cortical-basal ganglionic degeneration. In: Calne DB (ed) Neurodegenerative diseases, Saunders, Philadelpia, pp 877–894
38. Mathuranath PS, Xuereb JH, Bak T, Hodge JR (2000) Corticobasal ganglionic degeneration and/or frontotemporal dementia? A report of two overlap cases and review of literature. J Neurol Neurosurg Psychiatry 68:304–312

39. Mimura M, Oda T, Tsuchiya K, Kato M, Ikeda K, Hori K, Kashima H (2001) Corticobasal degeneration presenting with nonfluent primary progressive aphasia: a clinicopathological study. J Neurol Sci 183:19–26
40. Mitani K, Uchihara T, Tamaru F, Endo K, Tsukagoshi H (1993) Corticobasal degeneration: clinicopathological studies on two cases (in Japanese with English abstract). Clin Neurol (Tokyo) 33:155–161
41. Miyazaki H, Saito Y, Kijima Y, Akabane H, Tsuchiya K (1997) An autopsy case of corticobasal degeneration mimicking frontal Pick's disease (in Japanese with English abstract). No To Shinkei 49:277–282
42. Mizuno Y, Ozeki M, Iwata H, Takeuchi T, Ishihara R, Hashimoto N, Kobayashi H, Iwai K, Ogasawara S, Ukai K, Shibayama H (2002) A case of clinically and neuropathologically atypical corticobasal degeneration with widespread iron deposition. Acta Neuropathol 103:288–294
43. Mori H, Nishimura M, Namba Y, Oda M (1994) Coritcobasal degeneration: a disease with widespread appearance of abnormal tau and neurofibrillary tangles, and its relation to progressive supranuclear palsy. Acta Neuropathol 88:113–121
44. Munoz DG (1998) The pathology of Pick complex. In: Kertesz A, Munoz DG (eds), Pick's disease and Pick complex. Wiley-Liss, New York, pp 211–241
45. Murayama S, Inoue K, Kawakami H, Bouldin TW, Suzuki K (1991) A unique pattern of astrocytosis in the primary motor area in amyotrophic lateral sclerosis. Acta Neuropathol 82:456–461
46. Murayama S, Bouldin TW, Suzuki K (1992) Immunocytochemical and ultrastructural studies of upper motor neurons in amyotrophic lateral sclerosis. Acta Neuropathol 83:518–524
47. Nakano I, Donnenfeld H, Hirano A (1983) A neuropathological study of amyotrophic lateral sclerosis. With special reference to central chromatolysis and spheroid in the spinal anterior horn and some pathological changes of the motor cortex (in Japanese with English abstract). Neurol Med (Tokyo) 18:136–144
48. Nathan PW, Smith MC, Deacon P (1990) The corticospinal tract in man. Course and location of fibers at different segmental leves. Brain 113:303–324
49. Oda T, Kogure T, Tominaga I, Onaya M, Mimura M, Kato Y, Iwabuchi K, Haga C (1994) An autopsy case of progressive supranuclear palsy with echolalia showing psychiatric symptoms at the beginning (in Japanese). Seishinigaku 36:1159–1166
50. Oda T, Ikeda K, Akamatsu W, Iwabuchi K, Akiyama H, Kondo H, Seta K, Kato Y, Kogure T, Hori K, Tominaga I, Onaya M (1995) An autopsy case of corticobasal degeneration clinically misdiagnosed as Pick's disease (in Japanese with English abstract). Psychiatr Neurol Jpn 97:757–769
51. Oyanagi K, Tsuchiya K, Yamazaki M, Ikeda K (2001) Substantia nigra in progressive supranuclear palsy, corticobasal degeneration, and parkinsonism-dementia complex of Guam: specific pathological features. J Neuropathol Exp Neurol 60:393–402
52. Rebeiz JJ, Kolodny EH, Richardson EP Jr (1967) Corticodentatonigral degeneration with neuronal achromasia: a progressive disorder of late adult life. Trans Am Neurol Assoc 92:23–26
53. Rebeiz JJ, Kolodny EH, Richardson EP Jr (1968) Corticodentatonigral degeneration with neuronal achromasia. Arch Neurol 18: 20-33
54. Riley DE, Lang AE, Lewis A, Resch L, Ashby P, Hornykiewicz O, Black S (1990) Cortico-basal ganglionic degeneration. Neurology 40:1203-1212
55. Rinne JO, Lee MS, Thompson PD, Marsden CD (1994) Corticobasal degeneration. A clinical study of 36 cases. Brain 117:1183–1196
56. Rossor MN, Tyrrell PJ, Warrington EK, Thompson PD, Marsden CD, Lantos P (1999) Progressive frontal gait disturbance with atypical Alzheimer's disease and corticobasal degeneration. J Neurol Neurosurg Psychiatry 67:345–352
57. Schneider JA, Watts RL, Gearing M, Brewer RP, Mirra SS (1997) Corticobasal degeneration: Neuropathologic and clinical heterogeneity. Neurology 48:959–969
58. Su M, Yoshida Y, Hirata Y, Satoh Y, Nagata K (2000) Degeneration of the cerebellar dentate nucleus in corticobasal degeneration: neuropathological and morphometric investigations. Acta Neuropathol 99:365–370
59. Tolnay M, Probst A (2002) Frontotemporal lobar degeneration—tau as a pied piper? Neurogenetics 4:63–75
60. Tsuchiya K, Ikeda K (2002) Basal ganglia lesions in ' Pick complex': A topographic neuropathological study of 19 autopsy cases. Neuropathology 22:323–336
61. Tsuchiya K, Ikeda K, Watabiki S, Shiotsu H, Hashimoto K, Mitani K, Okiyama R, Sano M, Kondo H, Shimada H (1996) An unusual autopsy case of corticobasal degeneration—with special reference to clinicopathological differentiation from progressive supranuclear palsy and slowly progressive aphasia (in Japanese with English abstract). No To Shinkei 48:559–565
62. Tsuchiya K, Ikeda K, Uchihara T, Oda T, Shimada H (1997) Distribution of cerebral cortical lesions in corticobasal degeneration: a clinicopathological study of five autopsy cases in Japan. Acta Neuropathol 94:416–424
63. Tsuchiya K, Uchihara T, Oda T, Arima K, Ikeda K, Shimada H (1997) Basal ganglia lesions in corticobasal degeneration differ from those in Pick's disease and progressive supranuclear palsy: a topographic neuropathology of six autopsy cases. Neuropathology 17:208–216
64. Tsuchiya K, Miyazaki H, Ikeda K, Watabiki S, Kijima Y, Sano M, Shimada H (1997) Serial brain CT in corticobasal degeneration: radiological and pathological correlation of two autopsy cases. J Neurol Sci 152:23–29
65. Tsuchiya K, Arima K, Fukui T, Kuroiwa T, Haga C, Iritani S, Hirai S, Nakano I, Takemura T, Matsushita M, Ikeda K (1999) Distribution of basal ganglia lesions in Pick's disease with Pick bodies: a topographic neuropathological study of eight autopsy cases. Neuropathology 19:370–379
66. Tsuchiya K, Osawa E, Haga C, Watabiki S, Ikeda M, Sano M, Ooe K, Taki K, Ikeda K (2000) Constant involvement of the Betz cells and pyramidal tract in multiple system atrophy: a clinicopathological study of seven autopsy cases. Acta Neuropathol 99:628–636
67. Tsuchiya K, Ishizu H, Nakano I, Kita Y, Sawabe M, Haga C, Kuyama K, Nishinaka T, Oyanagi K, Ikeda K, Kuroda S (2001) Distribution of basal ganglia lesions in generalized variant of Pick's disease: a clinicopathological study of four autopsy cases. Acta Neuropathol 102:441–448
68. Tsuchiya K, Ikeda M, Hasegawa K, Fukui T, Kuroiwa T, Haga C, Oyanagi S, Nakano I, Matsushita M, Yagishita S, Ikeda K (2001) Distribution of cerebral cortical lesions in Pick's disease with Pick bodies: a clinicopathological study of six autopsy cases showing unusual clinical presentations. Acta Neuropathol 102:553–571
69. Tsuchiya K, Nakayama H, Iritani S, Arai T, Niizato K, Haga C, Matsushita M, Ikeda K (2002) Distribution of basal ganglia lesions in diffuse neurofibrillary tangles with calcification: a clinicopathological study of five autopsy cases. Acta Neuropathol 103:555–564
70. Tsuchiya K, Ikeda K, Mimura M, Takahashi M, Miyazaki H, Anno M, Shiotsu H, Akabane H, Niizato K, Uchihara T, Tominaga I, Nakano I (2002) Constant involvement of the Betz cells and pyramidal tract in amyotrophic lateral sclerosis with dementia: a clinicopathological study of eight autopsy cases. Acta Neuropathol 104:249–259
71. Uchihara T, Mitani K, Mori H, Kondo H, Yamada M, Ikeda K (1994) Abnormal cytoskeletal pathology peculiar to corticobasal degeneration is different from that of Alzheimer's disease or progressive supranuclear palsy. Acta Neuropathol 88:379–383
72. Uchihara T, Mizusawa H, Tsuchiya K, Kondo H, Oda T, Ikeda K (1998) Discrepancy between tau immunoreactivity and argyrophilia by the Bodian method in neocortical neurons of corticobasal degeneration. Acta Neuropathol 96:553–557

73. Wakabayashi K, Takahashi H (2004) Pathological heterogeneity in progressive supranuclear palsy and corticobasal degeneration. Neuropathology 24:79–86
74. Wakabayashi K, Oyanagi K, Makifuchi T, Ikuta F, Homma A, Homma Y, Horikawa Y, Tokiguchi S (1994) Corticobasal degeneration: etiopathological significance of the cytoskeletal alterations. Acta Neuropathol 87:545–553
75. Wakabayashi K, Mori F, Oyama Y, Kurihara A, Kamada M, Yoshimoto M, Takahashi H (2003) Lewy bodies in Betz cells of the motor cortex in a patient with Parkinson's disease. Acta Neuropathol 105:189–192
76. Wenning GK, Litvan I, Jankovic J, Granata R, Mangone CA, McKee A, Poewe W, Jellinger K, Ray Chaudhuri K, D'Olhaberriague L, Pearce RKB (1998) Natural history and survival of 14 patients with corticobasal degeneration confirmed at postmortem examination. J Neurol Neurosurg Psychiatry 64:184–189

J Neuropathol Exp Neurol

Vol. 64, No. 8
August 2005
pp. 665–674

ORIGINAL ARTICLE

Visualization of Newly Deposited tau in Neurofibrillary Tangles and Neuropil Threads

Tomohiro Miyasaka, PhD, Atsushi Watanabe, PhD, Yuko Saito, MD, Shigeo Murayama, MD, David M. A. Mann, PhD, Mineo Yamazaki, MD, Rivka Ravid, PhD, Maho Morishima-Kawashima, PhD, Kazuo Nagashima, MD, and Yasuo Ihara, MD

Abstract

Neurofibrillary tangles (NFTs) and neuropil threads (NTs), the major hallmark of Alzheimer disease (AD), are composed of the microtubule-associated protein tau that has undergone posttranslational modifications, including deamidation and isomerization on asparaginyl or aspartyl residues. Because such modifications represent protein aging, we generated 2 antibodies, TM4, specific for Asp-387 of tau, and iD387, specific for isoAsp-387 of tau, to investigate the evolution of NFTs and NTs. On Western blots of Sarkosyl-insoluble fractions, TM4 strongly labeled paired helical filament-tau (PHF-tau), whereas iD387 preferentially labeled PHF smear. Thus, it is reasonable to postulate that TM4-labeled tau (unmodified tau species) represents more recent deposition, and iD387-labeled tau (modified tau species) represents earlier deposition. Unexpectedly, TM4 immunostained even highly evolved NFTs, suggesting that deposition of newly produced tau continues until neuronal death. iD387 labeled the whole profile of NFTs up to distal dendritic branches, whereas TM4 staining was localized to particular portions of NFTs in proximal dendrites and neuronal perikarya. In NTs, TM4 preferentially labeled the outer portion, whereas iD387 intensely labeled the core portion. Based on TM4-positive NFT counts and total NFT counts, we speculate that NFTs in the human hippocampus are produced at a constant rate irrespective of the disease stage.

From the Department of Neuropathology (TM, MMK, YI), Faculty of Medicine, University of Tokyo, Tokyo, Japan; Laboratory of Molecular and Cellular Pathology (TM, KN), School of Medicine, Hokkaido University, Sapporo, Japan; Biomolecular Characterization Division (AW), Characterization Center, RIKEN (The Institute of Physical and Chemical Research), Japan; Department of Neuropathology (YS, SM), Tokyo Metropolitan Institute of Gerontology, Japan; Department of Medicine (DMAM), University of Manchester, Manchester, United Kingdom; Department of Neurology (MY), Nippon Medical School, Japan; The Netherlands Brain Bank (RR), Amsterdam, The Netherlands; and the Core Research for Evolutional Science and Technology (CREST) (YI), Japan Science and Technology Corporation (JST), Kawaguchi, Japan.

Send correspondence and reprint requests to: Yasuo Ihara, MD, Department of Neuropathology, Faculty of Medicine, University of Tokyo, 7-3-1 Hongo, Bunkyo-ku, Tokyo 113-0033, Japan; E-mail: yihara@m.u-tokyo.ac.jp

This work was supported in part by a Grant-in-Aid for Scientific Research on Priority Areas—Advanced Brain Science Project—from Ministry of Education, Culture, Sports, and Science and Technology, Japan (YI); and by a Research Grant for Longevity Sciences from the Ministry of Health and Welfare, Japan (MMK).

Key Words: Alzheimer disease, Tau, Protein aging, Isoaspartate, Neurofibrillary tangles, Neuropil threads.

INTRODUCTION

The abnormal intracytoplasmic inclusions referred to as neurofibrillary tangles (NFTs) and neuropil threads (NTs) are the major pathologic hallmark of tauopathies, including Alzheimer disease (AD), frontotemporal dementia, and parkinsonism linked to chromosome 17 (FTDP-17), and a number of other neurodegenerative diseases (1). Because areas forming NFTs and NTs correspond to those exhibiting neuronal loss in AD, it can be argued that the formation of these filamentous aggregates should be responsible for the neurodegeneration caused by AD and presumably by other tauopathies (2).

Various types of NFT are seen in AD brains: pretangles, intracellular (globose or flame-shaped) tangles, and extracellular (ghost) tangles (3). Pretangles may grow into globose or flame-shaped tangles (4, 5), which, in turn, are gradually converted to extracellular tangles, a tombstone of NFT-bearing neurons. The latter can be readily distinguished from intracellular tangles by their histologic and immunocytochemical staining characteristics (3, 6, 7). Because of their remarkable resistance to proteases (8–10), NFTs should be highly stable during the degeneration process and remain even after neuronal death. Thus far, only a few studies have focused on the temporal profile of NFT formation in vivo, probably as a result of the limited availability of markers for the aging of NFT.

The unit fibrils making up NFTs and NTs are called paired helical filaments (PHFs), which are 20 nm in diameter and constrict to 10 nm every 80 nm. The major component of PHFs is tau, a microtubule-associated protein that has a pivotal role in microtubule stabilization under physiological conditions (11). PHF and the tau deposited in AD brains exhibit striking characteristics: insolubility in Sarkosyl, sodium dodecyl sulfate (SDS), and urea, and smearing on SDS-PAGE (12–15). Various posttranslational modifications have been identified in tau purified from PHF-enriched fractions. Hyperphosphorylation is the best known and confers unusually slow mobility on SDS-PAGE (16–20). Ubiquitination has also been identified in the smeared tau (21). Deamidation of asparaginyl residues (Asn) and isomerization of aspartyl residues (Asp) are further modifications in the tau making up PHF smear (22).

The chemical reaction generating these can cause non-enzymatic cleavage leading to fragmentation of tau (23) and may further stabilize NFT and accelerate neurodegeneration.

Deamidation of Asn and isomerization of Asp in a protein occur spontaneously through cyclic succinimidyl intermediates, which can result in structural abnormalities and biologic dysfunction (Fig. 1) (24–27). In fact, if protein L-isoaspartyl methyltransferase, an enzyme that repairs isoAsp formation, is deleted, isomerized proteins progressively accumulate in the brain and fatal phenotypes emerge (28, 29). The tau in NFT has a rigid conformation and is not susceptible to proteases, and isoAsp-tau would accumulate with age. Thus, paired probes for Asp-tau and isoAsp-tau should provide a unique opportunity to distinguish between recent deposition and earlier deposition of tau in NFTs and NTs in the human brain (30). Thus, 2 antibodies that specifically recognize unmodified Asp-387 (numbered according to the 441-amino acid isoform of human tau) (31) and isomerized aspartyl residue (isoAsp) 387 were generated to visualize the distribution of recent and earlier deposited tau in AD brain.

MATERIALS AND METHODS

Subjects

Frozen brain tissues from control subjects and patients with AD were provided by Dr. A. Tamaoka (Tsukuba University Medical School) and Dr. D. J. Selkoe (Harvard Medical School). Paraffin-embedded blocks of the hippocampus from 53 subjects, including 24 patients with AD, were obtained from the Tokyo Examiner's Office (17 subjects), Tokyo Metropolitan Institute of Gerontology and Tokyo Metropolitan Geriatric Hospital (TMIG and TMG; 12 control subjects and 8 patients with AD), and Tsukuba University (16 patients with AD). The brains from TMIG and TMG were staged according to Braak and Braak (32). Vibratome sections from 15 AD brains were provided by Drs. S. Murayama and Y. Saito (Department of Neuropathology, TMIG), Dr. D. Mann (Clinical Neuroscience Research Group, University of Manchester, UK), and Dr. M. Yamazaki (Tokyo Metropolitan Institute for Neuroscience). Frozen specimens of 3 brains affected by the FTDP-17 P301L mutation (94-075, 94-079, and 96-113) and one brain affected by the R406W mutation (99-005), and paraffin-embedded sections from 3 P301L brains (97-075, 94-079, and 94-328) and one R406W brain (99-005) were from The Netherlands Brain Bank. Detailed pathologic information was provided previously (33).

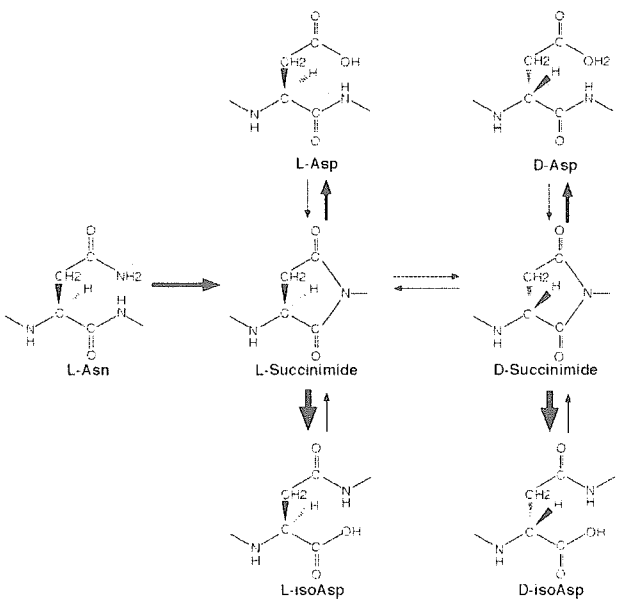

FIGURE 1. Schematic diagram of the isoAsp formation pathway through succinimidyl intermediate.

Antibodies

iD387 was raised against a synthetic peptide, T(isoD) HGAEIVYK (residues 386–395) (22). The specific IgG against the isoAsp peptide was purified by 2-step affinity purification; unbound fractions eluting from a TDHGAEIVYK-immobilized column were applied to a T(iD)HGAEIVYK-immobilized column. Bound fractions were eluted and obtained as iD387. TM4, anti-Asp-387 mouse monoclonal IgG, was raised against a synthetic peptide RENAKAKTDHGAEIVYKSPVV (residues 379–399) conjugated at its carboxyl terminus with bovine serum albumin (BSA). The antigen was emulsified in complete Freund's adjuvant and injected into mouse footpads. After 2 booster injections, lymphocytes obtained from inguinal lymph nodes were fused with PAI myeloma cells. Positive clones were selected by enzyme-linked immunosorbent assay (ELISA) and Western blotting. The specificities of these 2 antibodies were assessed by ELISA. For absorption, 2.5 μg/mL of each synthetic peptide were mixed with 2.5 μg/mL TM4 or 1:250-diluted iD387 and incubated at 37°C for 30 minutes. Other mouse monoclonal antibodies used here were TM2 (pan-tau monoclonal antibody, epitope: residues 368–386) (33), HT7 (antihuman tau, residues 159–163; Innogenetics, Zwijndrecht, Belgium), AT8 (antiphosphoSer-202 and phosphoThr-205-tau; Innogenetics), and AT100 (antiphosphoThr-212 and phosphoSer-214-tau; Innogenetics).

Tissue Fractionation and Western Blotting

Brain tissues were homogenized in Tris-saline (TS) containing a cocktail of protease inhibitors, as described previously (16). The homogenates were centrifuged at 540,000 × g for 20 minutes. The resultant TS-insoluble pellets were homogenized in 1% Sarkosyl and centrifuged again. The pellets obtained—Sarkosyl-insoluble fraction—were resuspended with 1% SDS followed by ultracentrifugation. Finally, the 1% SDS-insoluble pellets were suspended by vigorous sonication in SDS sample buffer (0.08 M Tris HCl, 2% SDS, 10% glycerol, 1% 2-mercaptoethanol, pH 6.8). Each fraction was subjected to Western blotting as described previously (33). Briefly, proteins separated on a 10% SDS-PAGE gel were electrotransferred onto a nylon membrane, which was incubated with each primary antibody. After incubation with HRP-conjugated

anti-IgG antibodies (Jackson Immunoresearch, West Grove, PA), bound antibodies were detected by enhanced chemiluminescence (ECL; Amersham, Buckingham, UK).

Enzyme-Linked Immunosorbent Assay

ELISA plates (Nunc-Immunoplate; Nunc A/S, Roskilde, Denmark) were coated with 0.5 μg of each synthetic peptide and incubated with appropriately diluted primary antibodies. After brief washing, bound antibodies were detected with HRP-conjugated antimouse or antirabbit IgG and the color was developed by the TMB Microwell Peroxidase Substrate system (Kirkegaard and Perry Laboratories, Gaithersburg, MD).

Immunocytochemistry

Paraffin-embedded sections were immunostained as described previously (33). To determine the optimal staining conditions for these antibodies, various pretreatments were tested, including pretreatment with 0.5% Triton X-100, target retrieval solution (DakoCytomation, Carpinteria, CA), 95% formic acid, by autoclaving, and pretreatment by autoclaving followed with formic acid. We found that treatment with 95% formic acid for 4 minutes provides the optimum for AT8 staining, and treatment by autoclaving at 120°C for 7 minutes followed with 95% formic acid for 4 minutes for TM2-, TM4-, and iD387-staining (34). After pretreatment, sections were incubated with primary antibodies overnight at room temperature, incubated with biotinylated antimouse or antirabbit IgG (Vector Laboratories, Inc., Burlingame, CA), and finally with avidin and biotinylated HRP (Vectastain ABC kit; Vector Laboratories, Inc.). Bound antibodies were visualized with 3,3′-diaminobenzidine (DAB) in the presence of hydrogen peroxide, and the DAB-developed sections were briefly counterstained with hematoxylin. Semiquantification of NFT was performed as described previously (34). TM2- or TM4-positive NFTs were counted, and their numbers were averaged across 3 nonselected areas of 3.2 mm^2.

For confocal microscopy, 30- to 50-μm thick vibratome sections from AD cerebral cortex were pretreated with 95% formic acid followed by incubation with primary antibodies. This treatment provided better conditions for the staining of tau inclusions with TM4 and iD387, compared with no treatment or 0.5% Triton X-100 treatment (data not shown). Bound antibodies were visualized with Alexa 488-conjugated antimouse IgG or Alexa 568-conjugated antirabbit IgG (Molecular Probes, Inc., Eugene, OR). When necessary, lipofuscin autofluorescence was eliminated with Sudan Black B, as described previously (35). Specimens were observed under a Zeiss Axioskop microscope (Carl Zeiss Inc., Thornwood, NY) equipped with the Lasersharp2000 software (Bio-Rad Laboratories).

RESULTS

Characterization of Asp-387-Specific, and isoAsp-387-Specific Antibodies

Three major deamidation/isomerization sites, Asp-193, Asn-381, and Asp-387, were previously identified in the PHF-smear (22) (Fig. 1). iD387 was raised against a synthetic peptide containing isoAsp-387 (Fig. 2A). On the ELISA plate, iD387 preferentially reacted with the isoAsp peptide, but scarcely with the unmodified Asp peptide (Fig. 2B). However, this antibody crossreacted to some extent with dextro-isoAsp-387 (diD387) peptide, a minor product in the isoAsp formation reaction (36) (Fig. 1). The Asn-381-modified peptide had no effect on the reactivities of these antibodies (data not shown). In contrast, TM4, raised against residues 379–399 (Fig. 2A), reacted exclusively with unmodified Asp-387 peptide and not with isoAsp-387 peptide (Fig. 2B). The effect of preabsorption was also assessed by Western blotting (Fig. 2C). TM4 labeling of recombinant tau was greatly reduced by preabsorption with L-Asp peptide but not with L-isoAsp peptide. Thus, TM4 specifically labels unmodified Asp-387-containing tau. Furthermore, the specificity of these 2 antibodies was examined by immunocytochemistry. Combined treatment by autoclaving and formic acid was found to be the most effective for immunostaining with TM2, TM4, and iD387 (data not shown). Under this condition, TM4 intensely labeled NFTs in AD brains, staining being abolished by preabsorption with Asp-peptide (Fig. 2D). Despite strong labeling of normal (soluble) tau on Western blots, TM4 does not obviously stain unaffected neurons in which abundant normal tau should exist. This may reflect the characteristics of tau: unmodified tau is normally unfolded and susceptible to formalin fixation, whereas modified (especially phosphorylated) tau has a particular conformation, which is resistant to fixation (37). On the other hand, preabsorption with L-isoAsp peptide completely eliminated the immunoreactivity of iD387 for NFTs (Fig. 2D).

Western blotting of Insoluble Fractions Using Asp-387- and isoAsp-387-Specific Antibodies

To assess the extent of isoAsp-387 formation, Sarkosyl-insoluble and SDS-insoluble fractions from control and AD brains were subjected to Western blotting using TM4, iD387, and other tau antibodies. The Sarkosyl-insoluble tau in AD brains is characterized by the presence of PHF-tau and PHF smear on the blots (21).

TM2, the epitope of which is located in residues 368–386 (Fig. 2A), intensely labeled PHF smear in the Sarkosyl-insoluble and SDS-insoluble fractions from AD brain (Fig. 3A). HT7, AT8, and AT100, the epitopes of which are located in the aminoterminal half or midportion of tau (see "Materials and Methods" for detailed information), strongly labeled 3 (or 4) bands of PHF-tau, but only faintly labeled PHF smear, especially the smear in the SDS-insoluble fraction (Fig. 3B–D). This indicates that the aminoterminal portion is lost in PHF smear and that AT8 can detect only a fraction of detergent-insoluble tau. This is consistent with previous reports on the selective concentration of the carboxyl-third of tau in PHF smear (21, 22).

As noted, PHF-tau was recovered exclusively in the Sarkosyl-insoluble, SDS-soluble fraction, whereas PHF smear was left in the SDS-insoluble fraction. The SDS-insoluble smear stayed in the stacking gel, whereas the SDS-soluble smear entered the separating gel and extended from high-molecular-weight to low-molecular-weight regions (Fig. 3A). These data suggest that filaments made of PHF smear are more resistant to SDS than those of PHF-tau. Such insoluble tau was